Correlation Plenoptic Imaging

Francesco Di Lena
Gruppo 5 / Gruppo 4

Congresso della Sezione INFN e del Dipartimento interateneo di Fisica di Bari
22/06/2021

The future is Quantum.

The Second Quantum Revolution is unfolding now, exploiting the enormous advancements in our ability to detect and manipulate single quantum objects. The Quantum Flagship is driving this revolution in Europe.

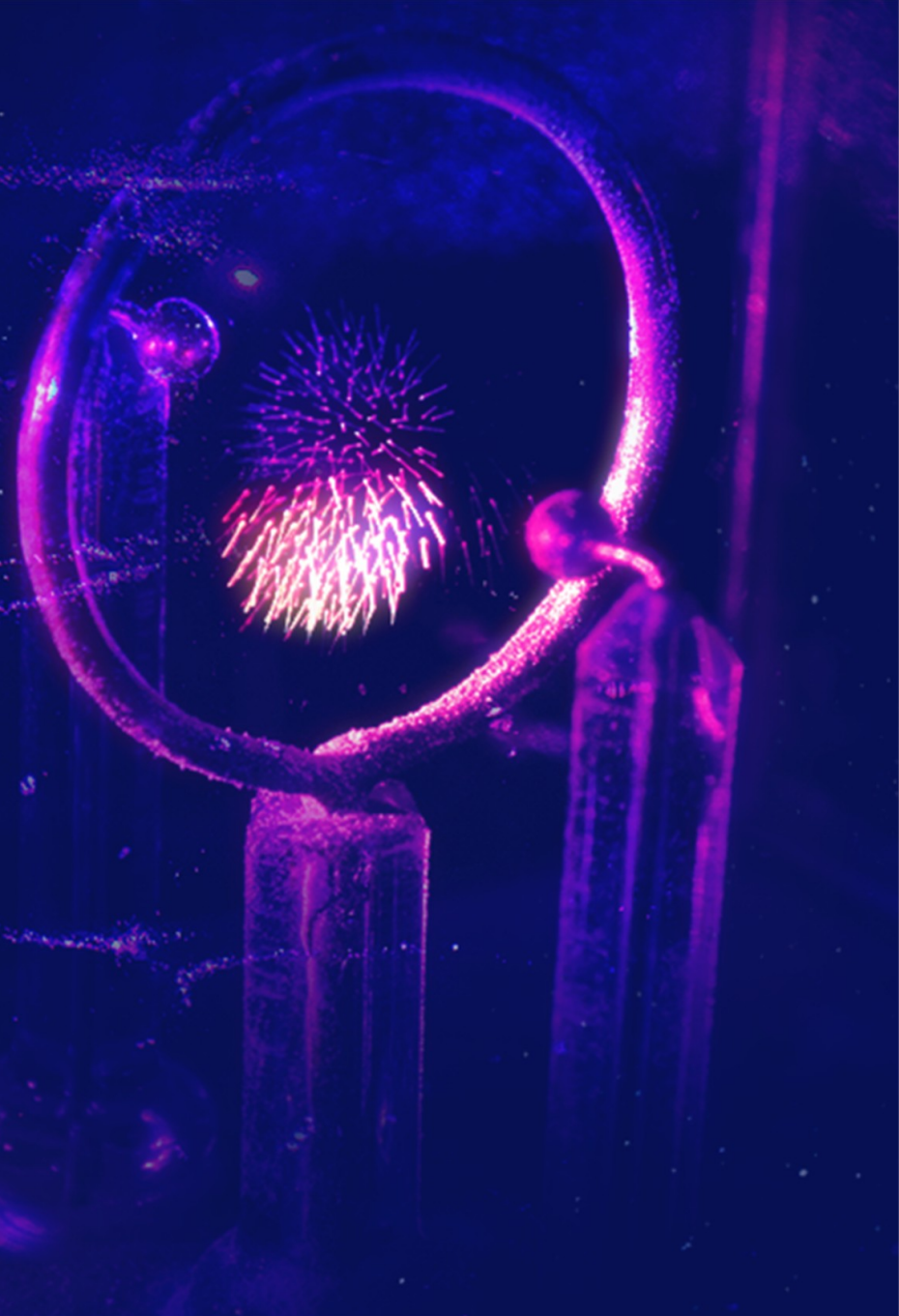

Quantum technologies 2.0:

- Quantum communication
- Quantum computation
- Quantum simulation
- Quantum Metrology/Sensing/IMAGING

Why Correlation Plenoptic Imaging?

Standard plenoptic imaging (SPI)

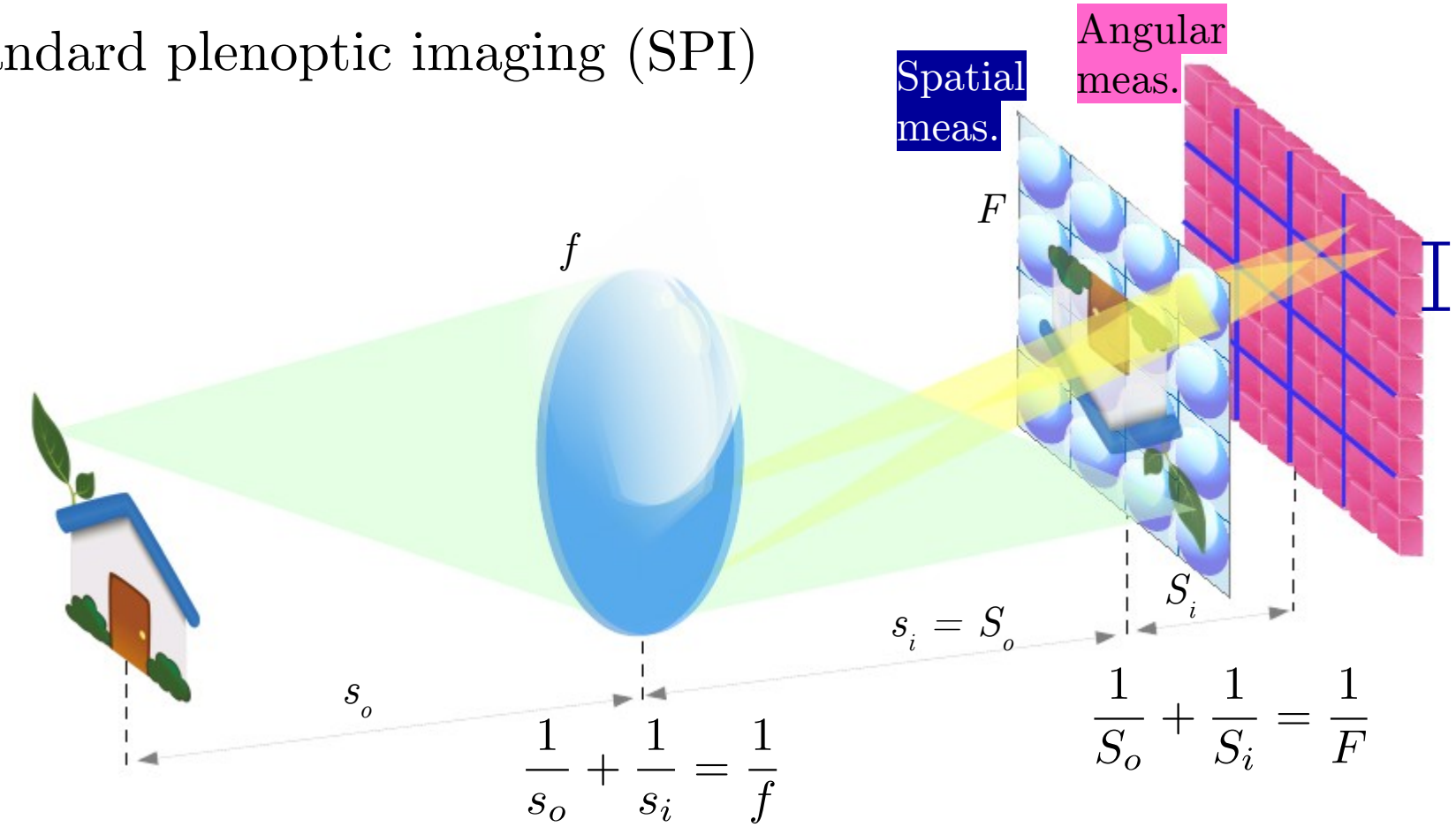

N_u = number of pixels for the angular measurement

E. H. Adelson and J. Y. Wang, IEEE transactions on pattern analysis and machine intelligence, 14, 99 (1992).
R. Ng, et al., Stanford University Computer Science Tech Report CSTR 2005-02, (2005).

Why Correlation Plenoptic Imaging?

Standard plenoptic imaging (SPI)

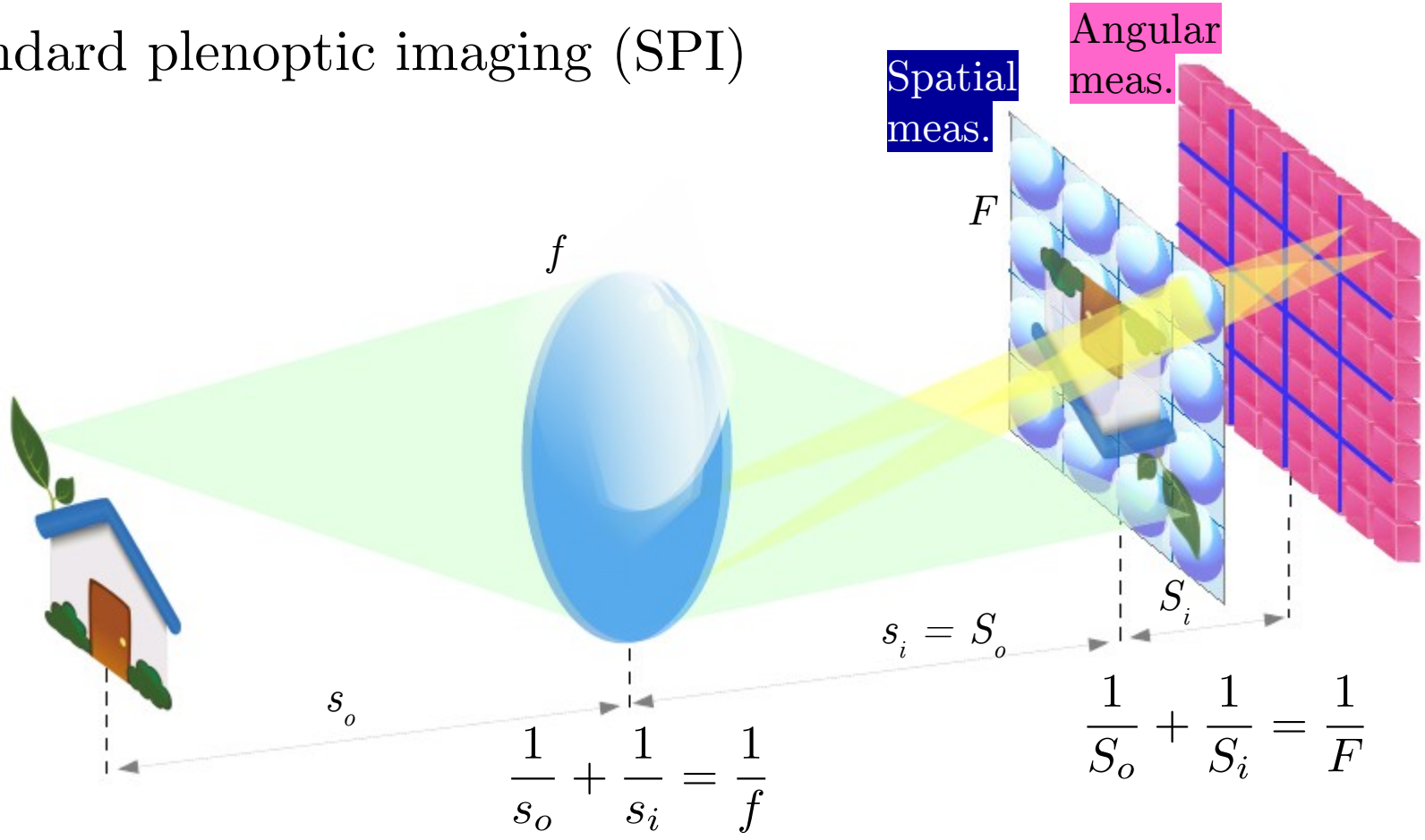

Acquired data

E. H. Adelson and J. Y. Wang, IEEE transactions on pattern analysis and machine intelligence, 14, 99 (1992).
R. Ng, et al., Stanford University Computer Science Tech Report CSTR 2005-02, (2005).

Why Correlation Plenoptic Imaging?

Standard plenoptic imaging (SPI)

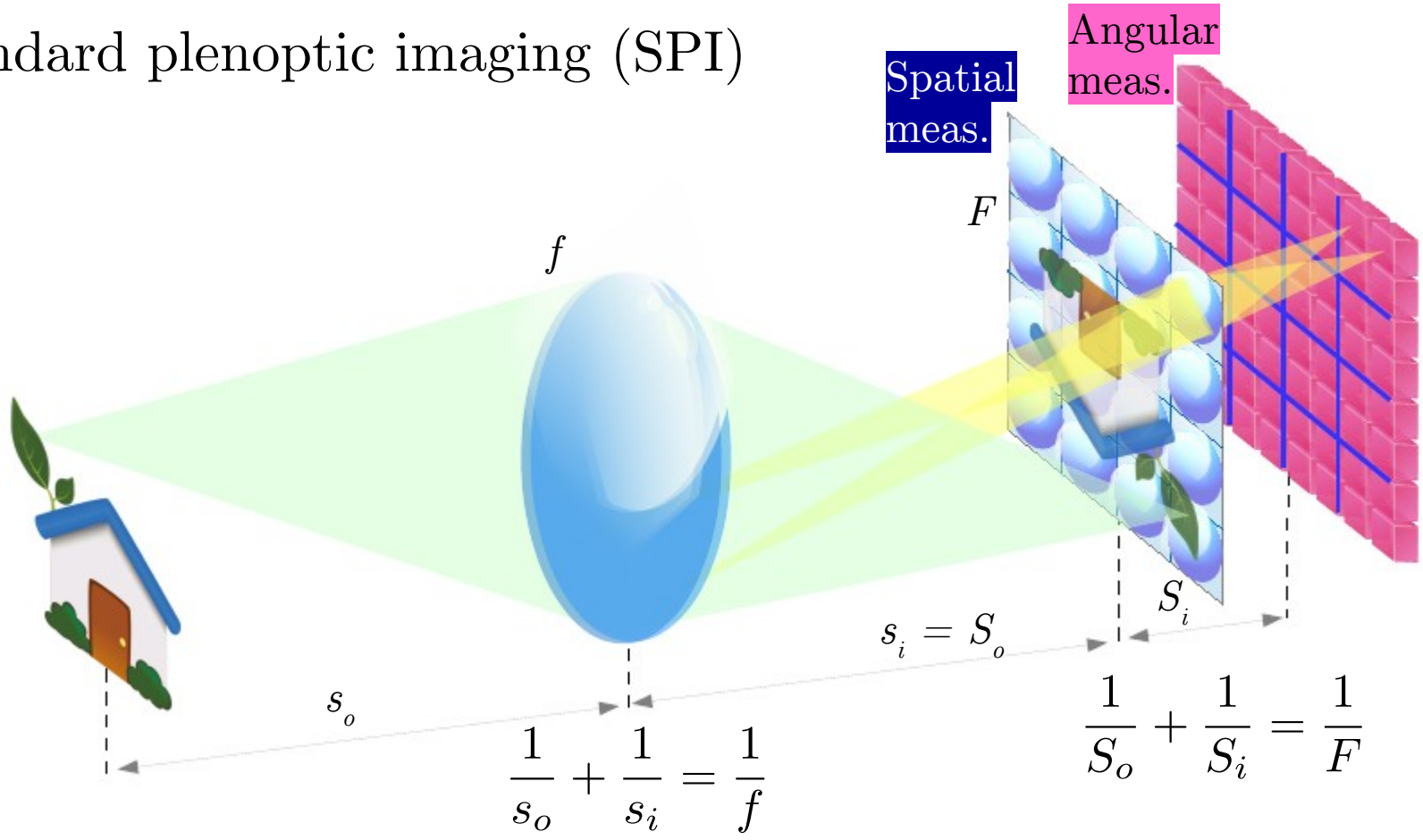

Post processing closest refocus

E. H. Adelson and J. Y. Wang, IEEE transactions on pattern analysis and machine intelligence, 14, 99 (1992).
R. Ng, et al., Stanford University Computer Science Tech Report CSTR 2005-02, (2005).

Why Correlation Plenoptic Imaging?

Standard plenoptic imaging (SPI)

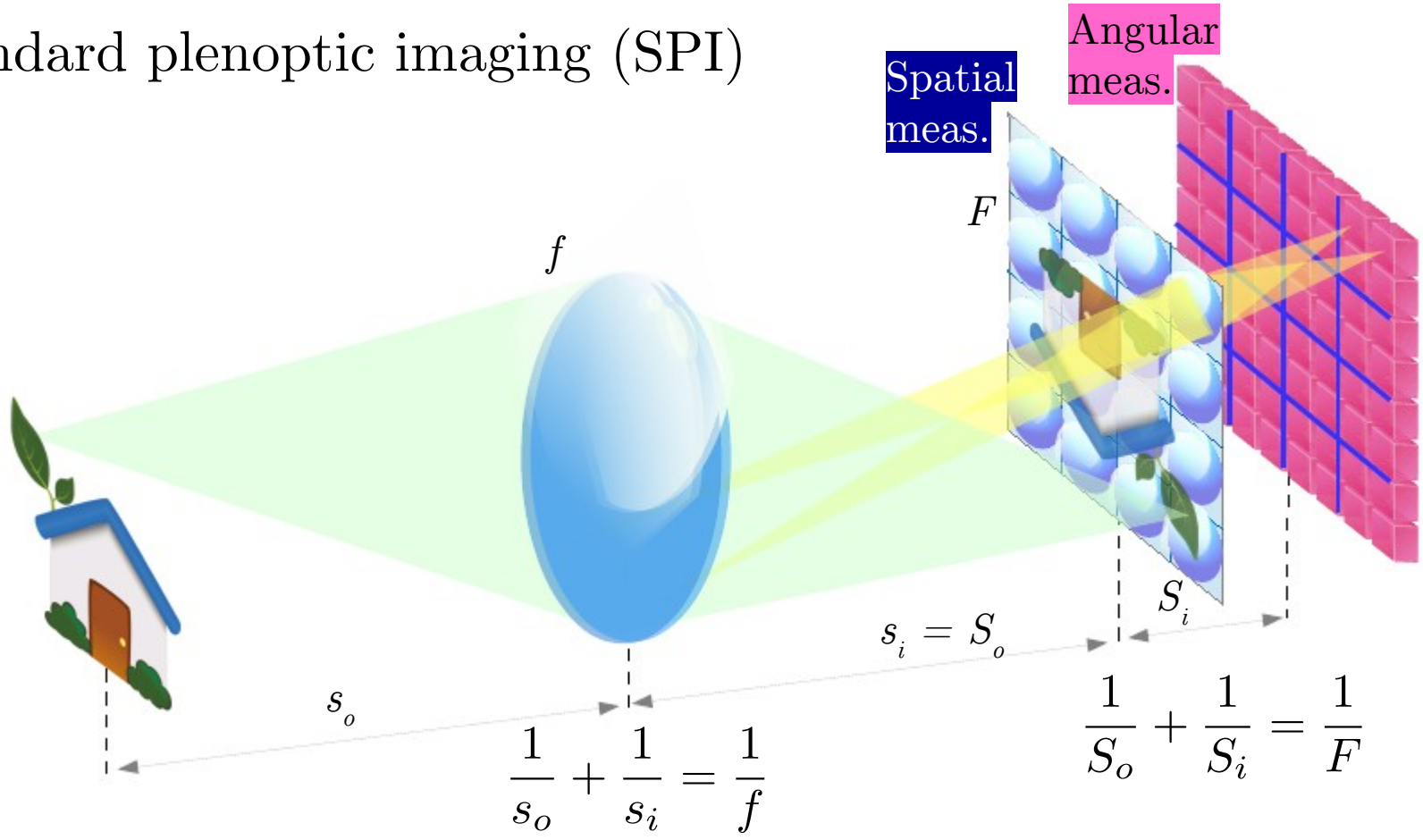

Post processing farthest refocus

E. H. Adelson and J. Y. Wang, IEEE transactions on pattern analysis and machine intelligence, 14, 99 (1992).
R. Ng, et al., Stanford University Computer Science Tech Report CSTR 2005-02, (2005).

Why Correlation Plenoptic Imaging?

Standard plenoptic imaging (SPI)

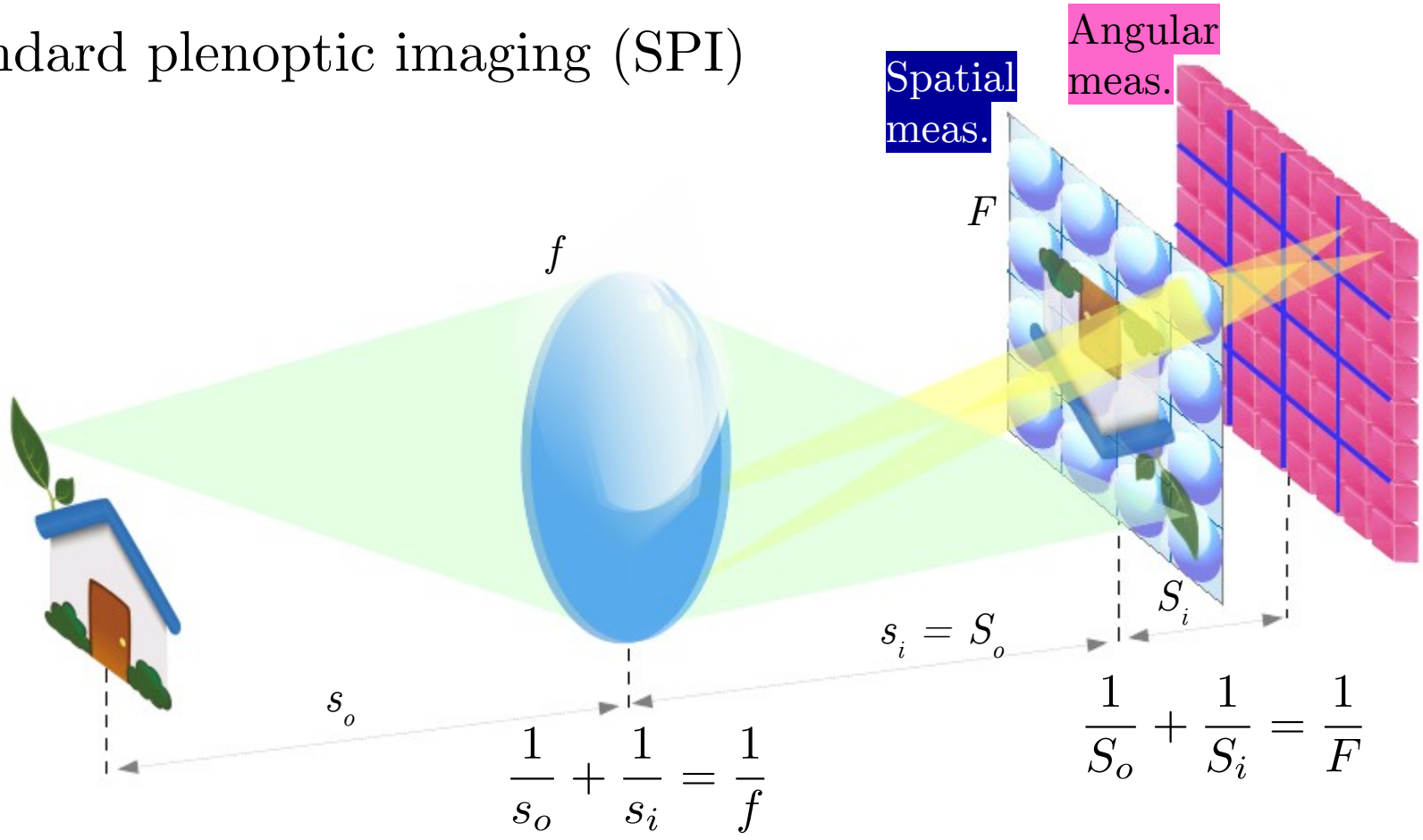

Extended depth of field (DOF)

E. H. Adelson and J. Y. Wang, IEEE transactions on pattern analysis and machine intelligence, 14, 99 (1992).
R. Ng, et al., Stanford University Computer Science Tech Report CSTR 2005-02, (2005).

Why Correlation Plenoptic Imaging?

Standard plenoptic imaging (SPI)

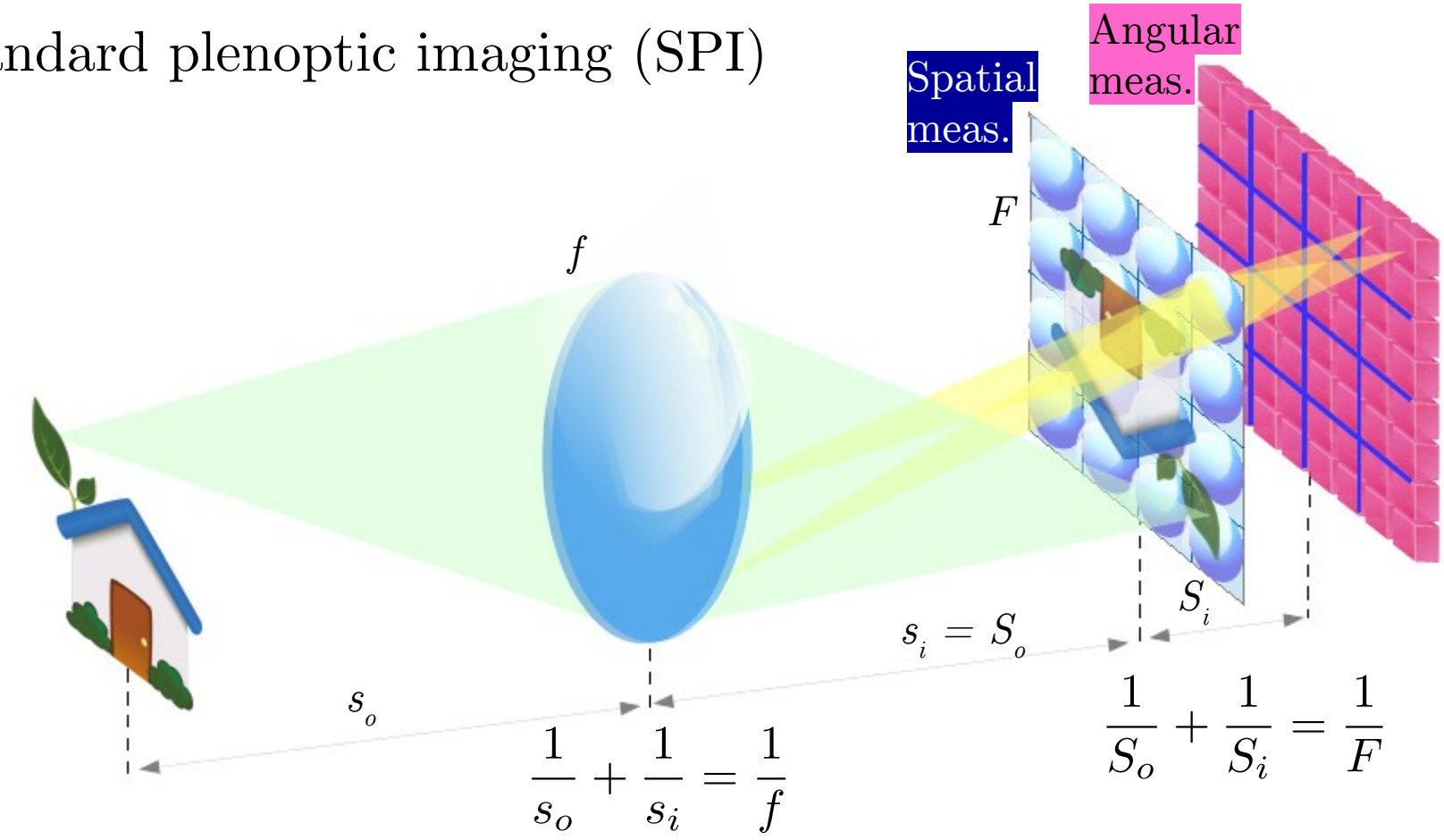

Limit of standard plenoptic imaging:

- No diffraction limited resolution
- Small change of perspective for 3D imaging.
- Strong trade-off between resolution and maximum achievable (DOF).

raytrix.de

- 3D Optical Inspection
- 3D Fluid Mechanics (PTV)

E. H. Adelson and J. Y. Wang, IEEE transactions on pattern analysis and machine intelligence, 14, 99 (1992).
R. Ng, et al., Stanford University Computer Science Tech Report CSTR 2005-02, (2005).

Can correlation help?

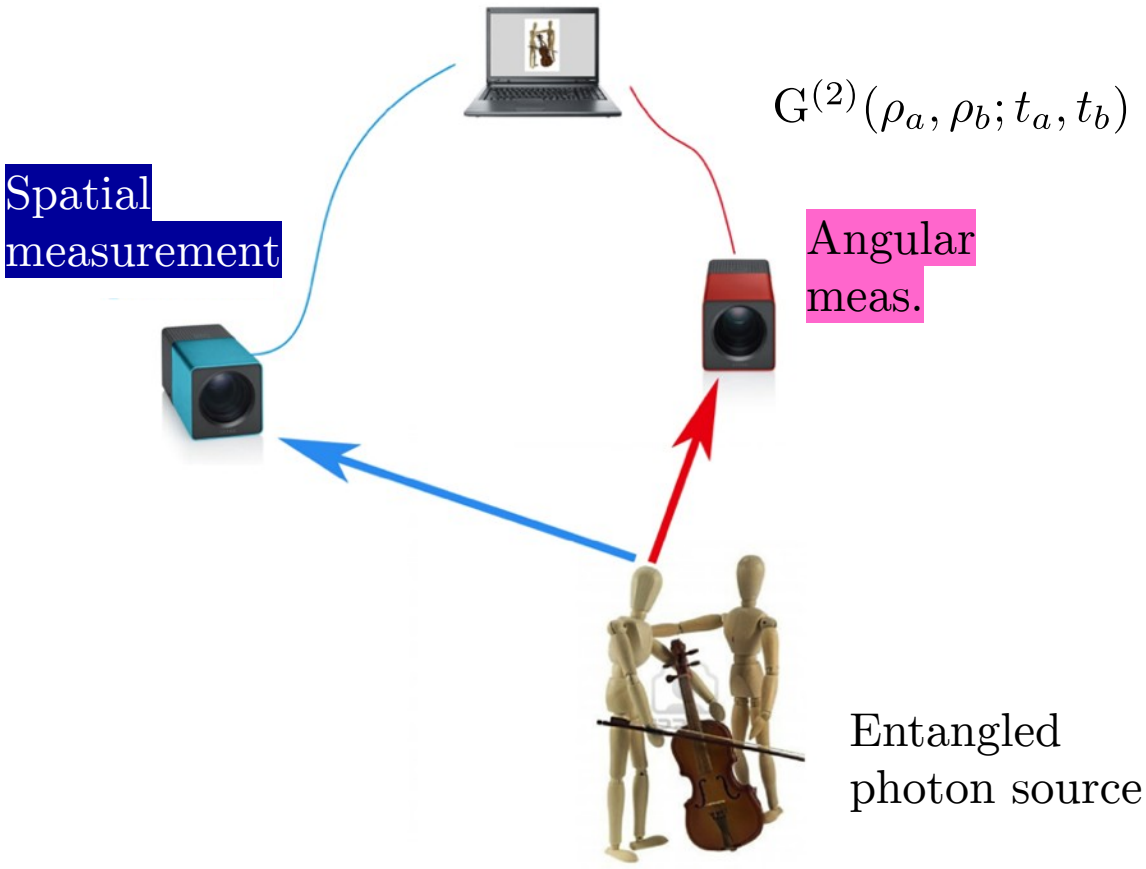

$$G^{(2)}(\rho_a, \rho_b; t_a, t_b) = < E_a^{(-)}(\rho_a, t_a) E_b^{(-)}(\rho_b, t_b) E_a^{(+)}(\rho_a, t_a) E_b^{(+)}(\rho_b, t_b) >$$

($E_j \rightarrow$ Field at the detectors j)

Correlation Plenoptic Imaging (CPI): extracts information contained in correlated light. → Refocusing and 3D imaging without losing resolution and wide change of perspective.

Can correlation help?

$$G^{(2)}(\rho_a, \rho_b; t_a, t_b) = < I_a >< I_a > + < \Delta I_a \Delta I_b >$$

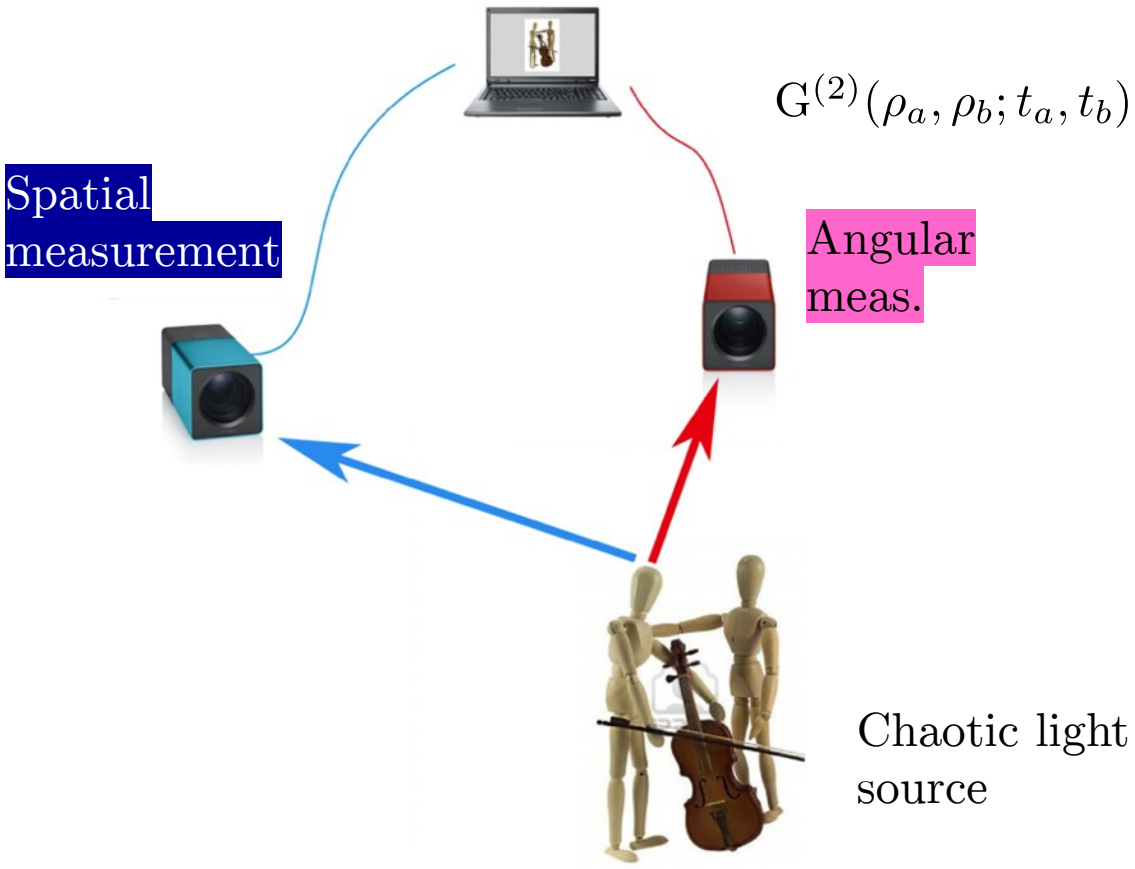

Correlation Plenoptic Imaging (CPI): extracts information contained in correlated light. → Refocusing and 3D imaging without losing resolution and wide change of perspective.

Can correlation help?

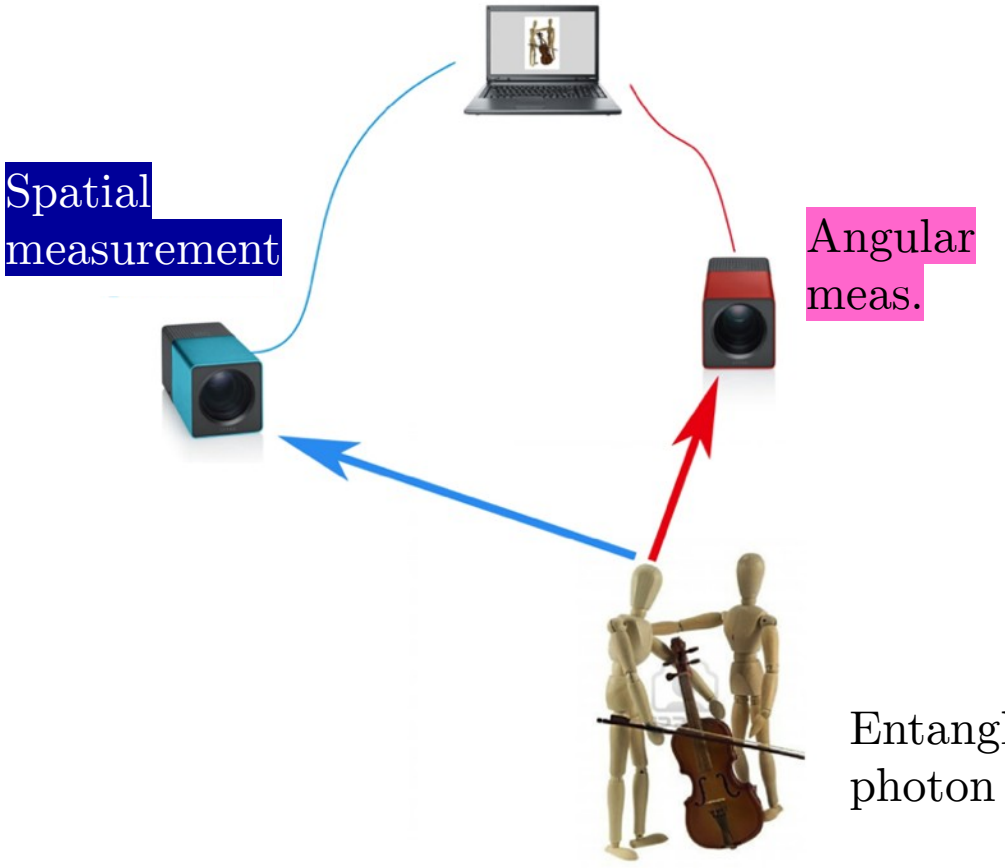

Entangled photons

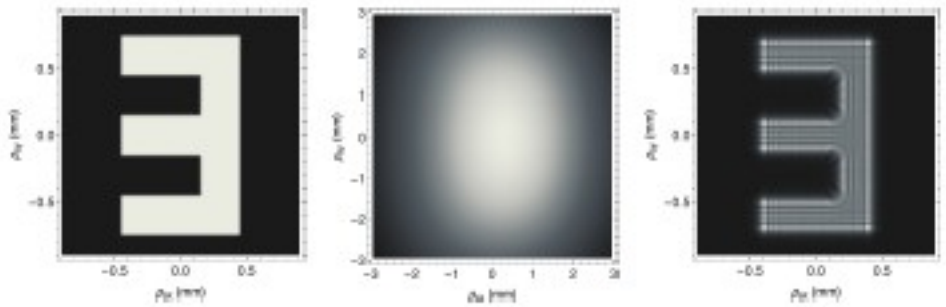

F.V. Pepe et al., Technologies 4, 17 (2016)

Correlation Plenoptic Imaging (CPI): extracts information contained in correlated light. → Refocusing and 3D imaging without losing resolution and wide change of perspective.

Were we are

DOF vs. resolution trade-off

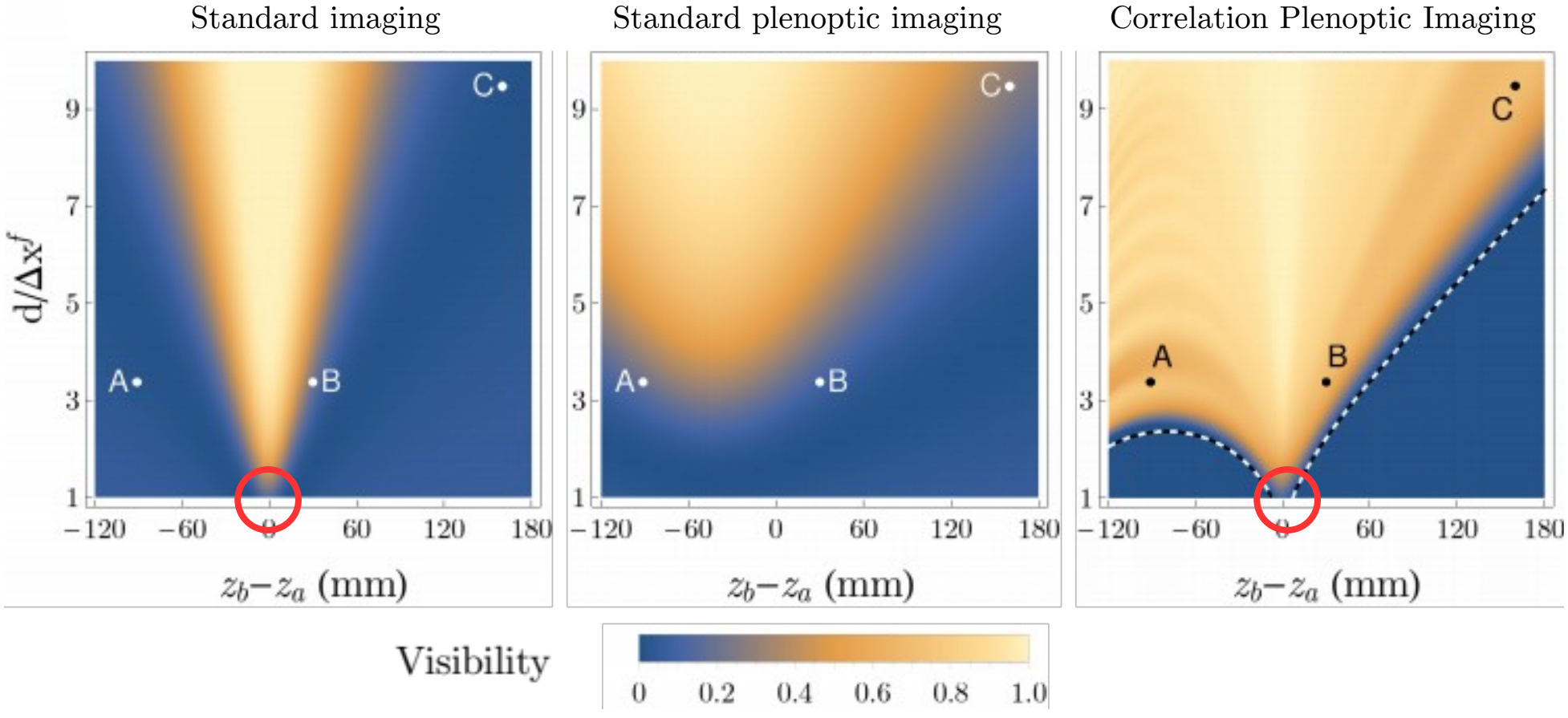

CPI enables refocusing in a much wider range than standard imaging and PI, while keeping the resolution of standard imaging!

Challenging

Scientific

1. Development of new approaches to encode images in light correlations.
2. CPI with challenges light sources, including natural ones.

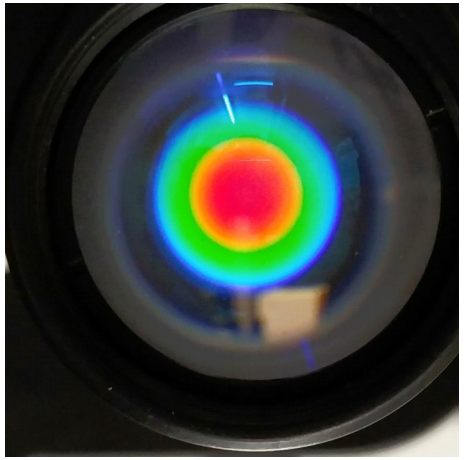

SPDC source

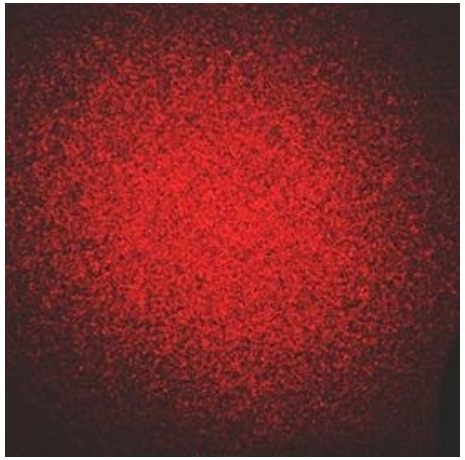

Chaotic source

Technological

1. Speed-up of acquisition and elaboration.
2. Adaptation of CPI to specific imaging tasks.
3. Patents, prototypes...

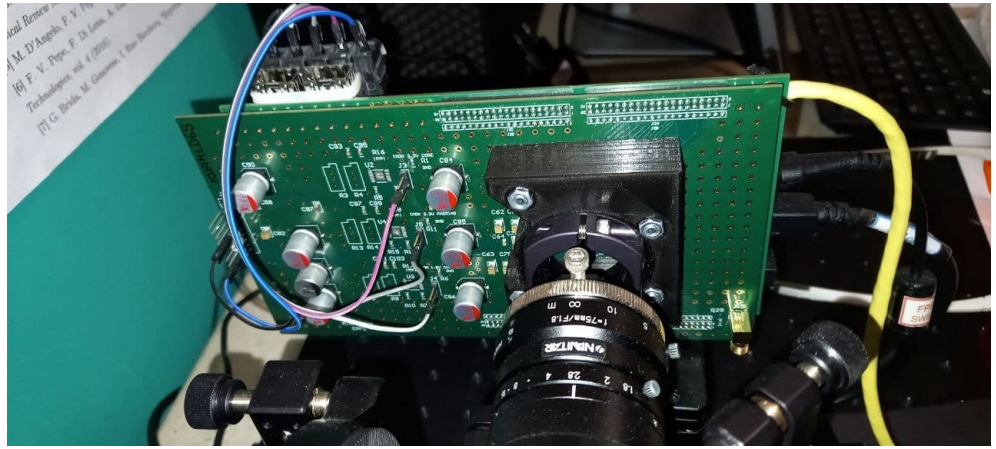

SPAD array camera

INFN ongoing projects

PICS4ME

Qu3D

INTEFF-TOPMICRO

PoC MISE

PICS4ME*

Plenoptic Imaging with Correlations for Microscopy and 3D Imaging Enhancement

CSN5 Ricerca Tecnologica

1. Design, development and characterization, and optimization of the Correlation Plenoptic Microscope CPM prototype
2. Comparison of the CPM with 3D microscopy systems (e.g., confocal microscopy), to demonstrate its effectiveness in several applicative scenarios
3. Data analysis optimization and 3D reconstruction algorithms
4. Explore novel protocols for SNR optimization
5. CPI with low-coherence sources

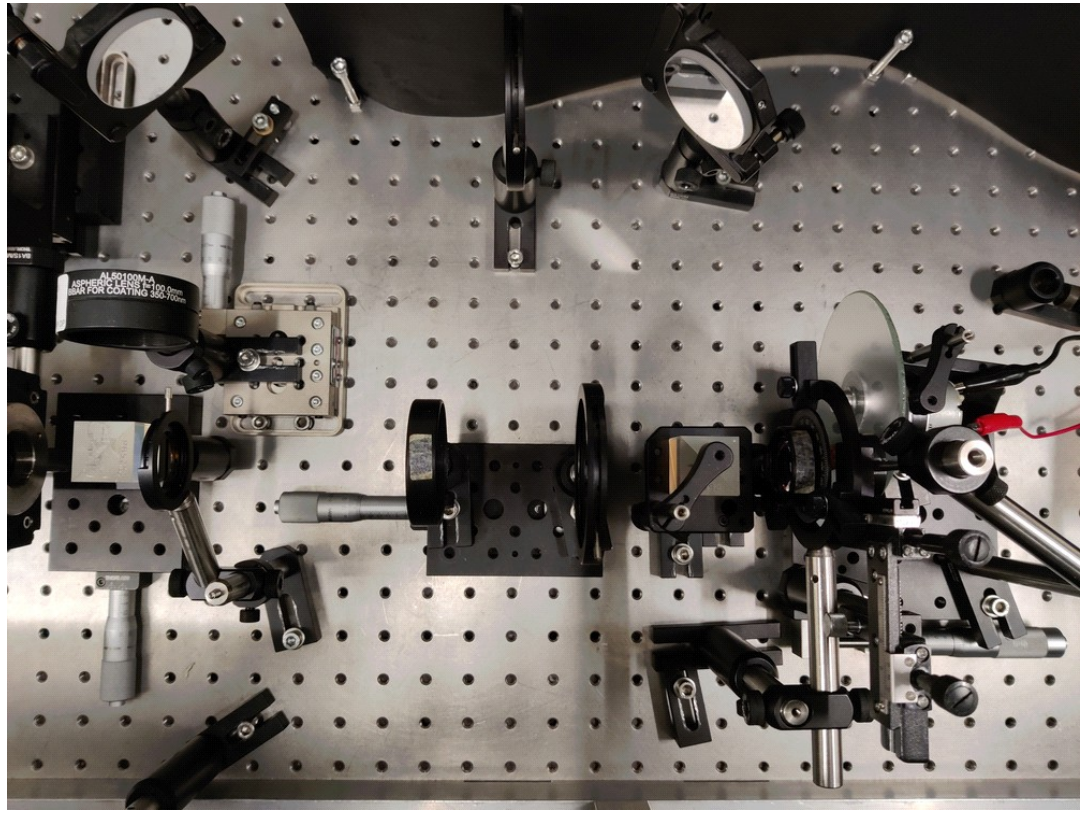

*Legacy of the Project PICS (young researcher grant CNS5 2017-2019, PI: Francesco Pepe)

Correlation Plenoptic Microscope

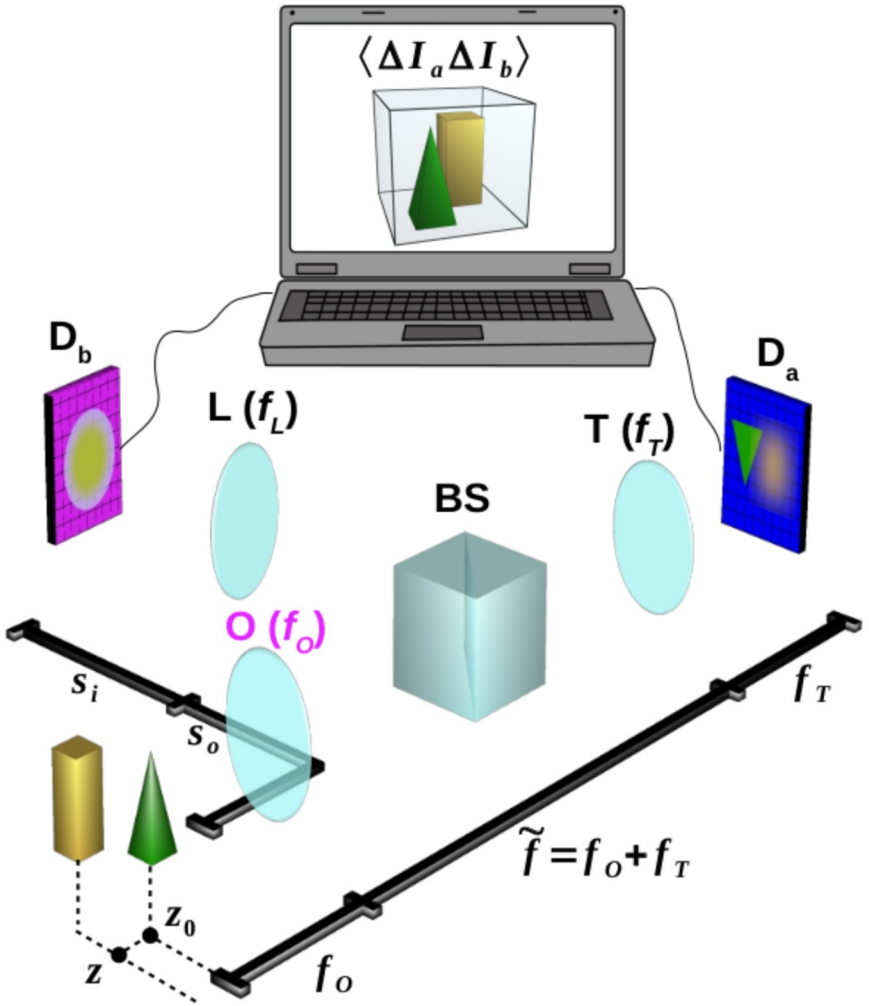

- A. Scagliola, F. Di Lena, A. Garuccio, M. D'Angelo, and F. V. Pepe, Physics Letters A, p. 126472, 2020.
- Paper on the experiment in preparation!

Correlation Plenoptic Microscope

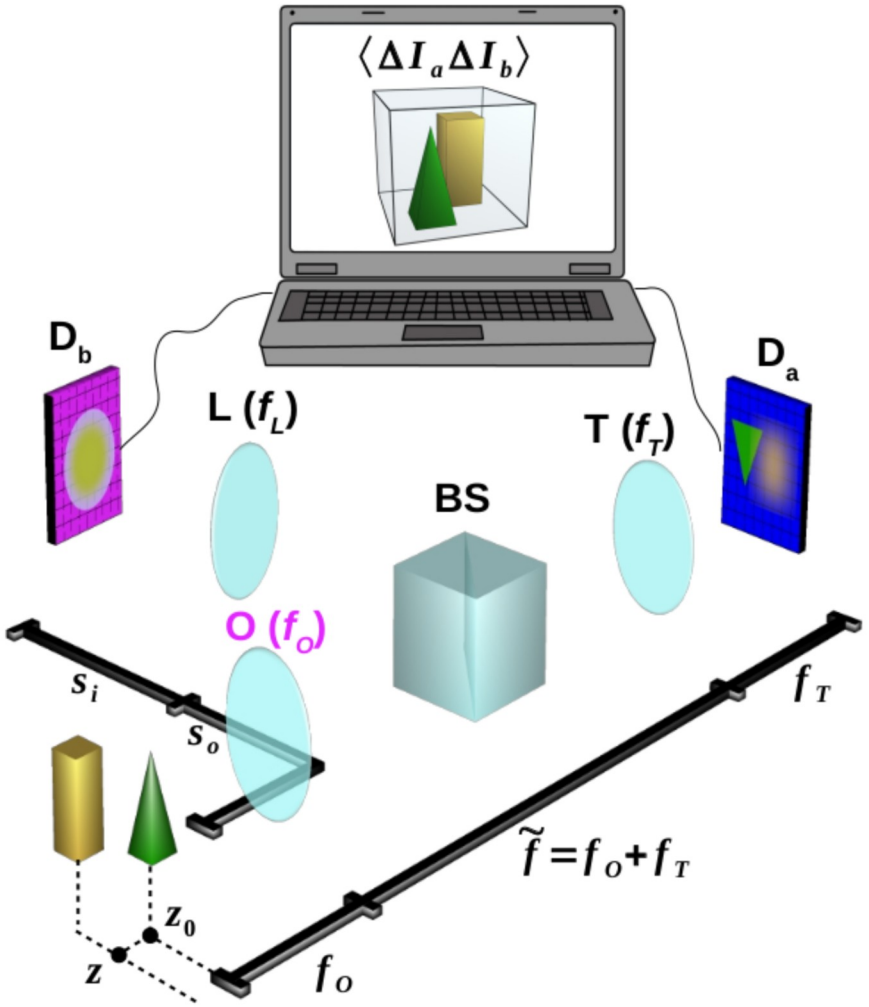

Acquired image at focus plane: z = 0

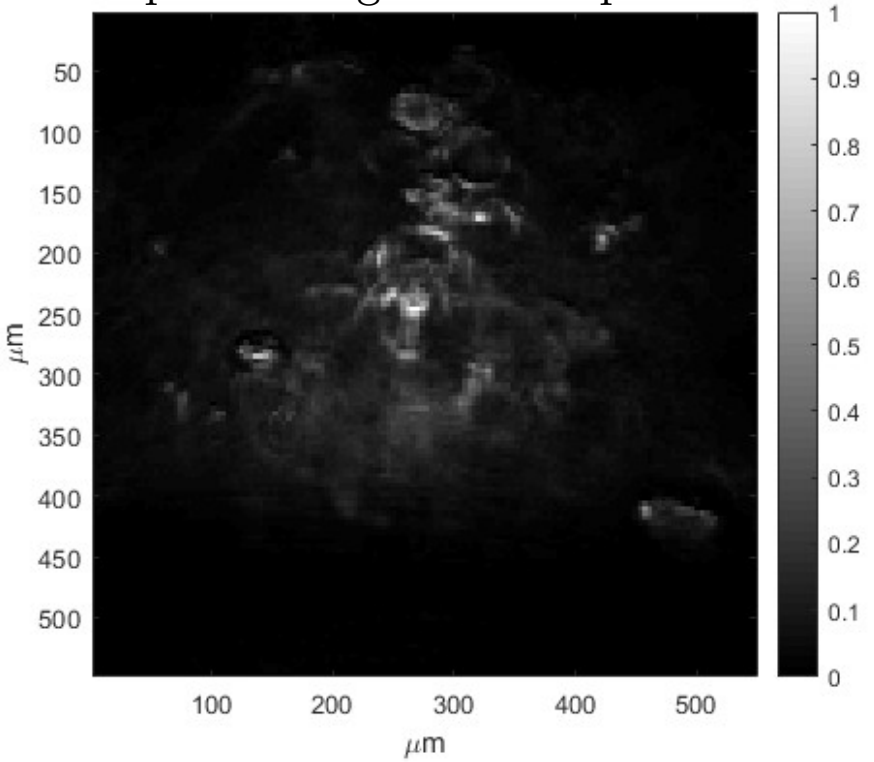

- A. Scagliola, F. Di Lena, A. Garuccio, M. D'Angelo, and F. V. Pepe, Physics Letters A, p. 126472, 2020.
- Paper on the experiment in preparation!

Correlation Plenoptic Microscope

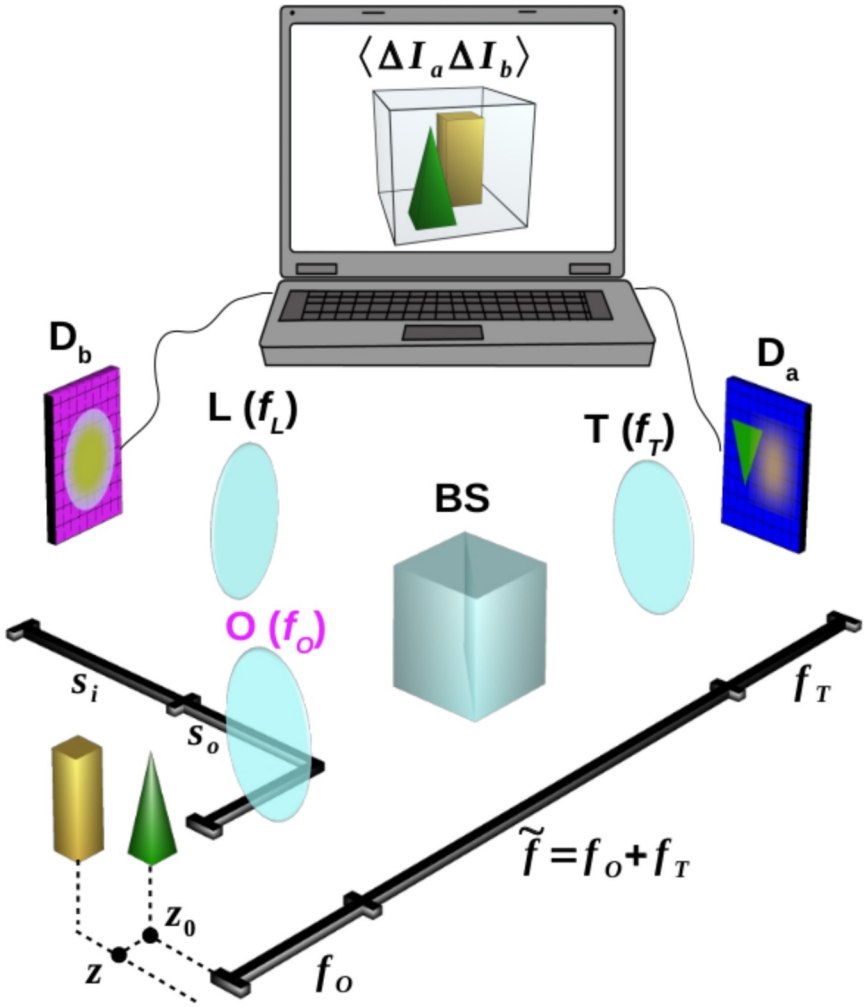

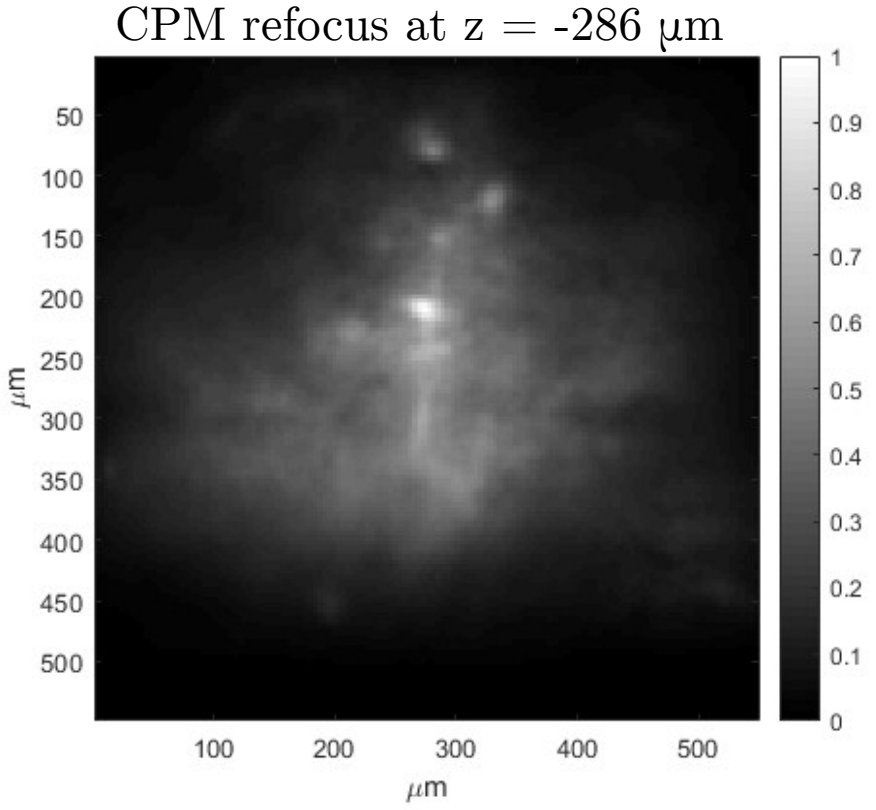

Different axial planes of a 3D sample (starch in gel) has been refocused in post-processing.

- A. Scagliola, F. Di Lena, A. Garuccio, M. D'Angelo, and F. V. Pepe, Physics Letters A, p. 126472, 2020.
- Paper on the experiment in preparation!

Correlation Plenoptic Microscope

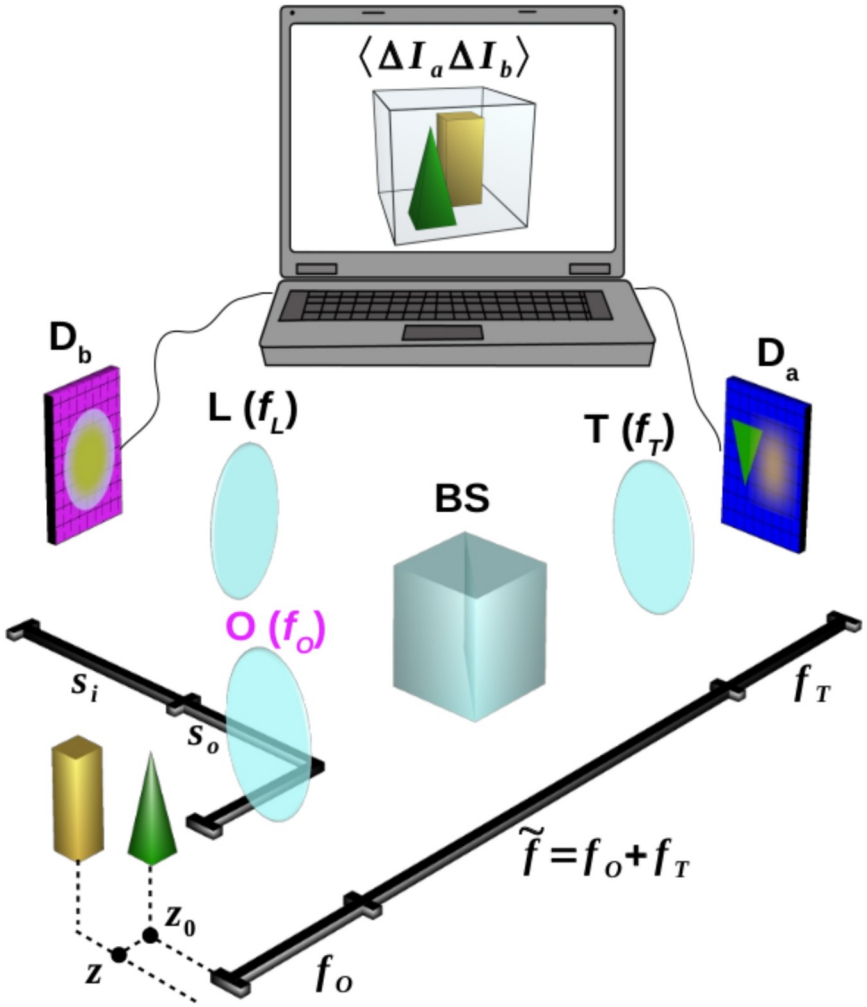

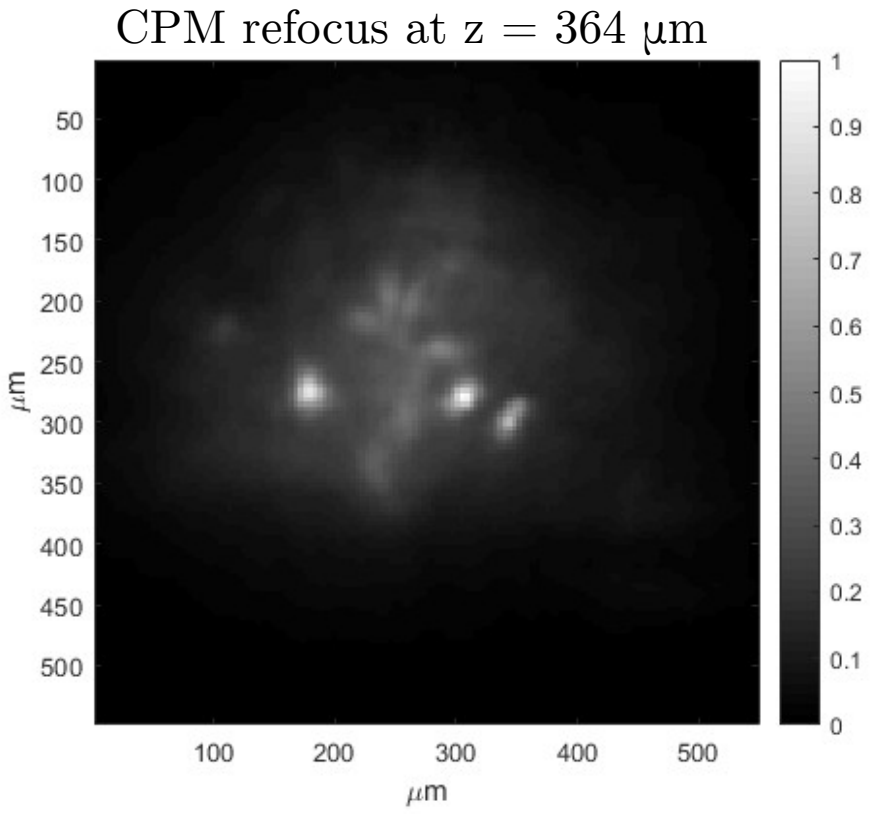

Different axial planes of a 3D sample (starch in gel) has been refocused in post-processing.

- A. Scagliola, F. Di Lena, A. Garuccio, M. D'Angelo, and F. V. Pepe, Physics Letters A, p. 126472, 2020.
- Paper on the experiment in preparation!

Differential CPI

CPI

$$\Sigma(x_a) = \int \delta I_A(\alpha x_a + \beta x_b)\delta I_B(x_b)\, dx_b$$

Differential CPI

$$\Sigma_{\text{diff}}(x_a) = \Sigma(x_a) - \frac{\int dx_b \, \langle \delta I_A(\alpha x_a + \beta x_b)\, \delta I_{A,\text{tot}} \rangle \langle \delta I_{A,\text{tot}}\, \delta I_B(x_b) \rangle}{\langle (\delta I_{A,\text{tot}})^2 \rangle}$$

Refocus at z = 364 μm

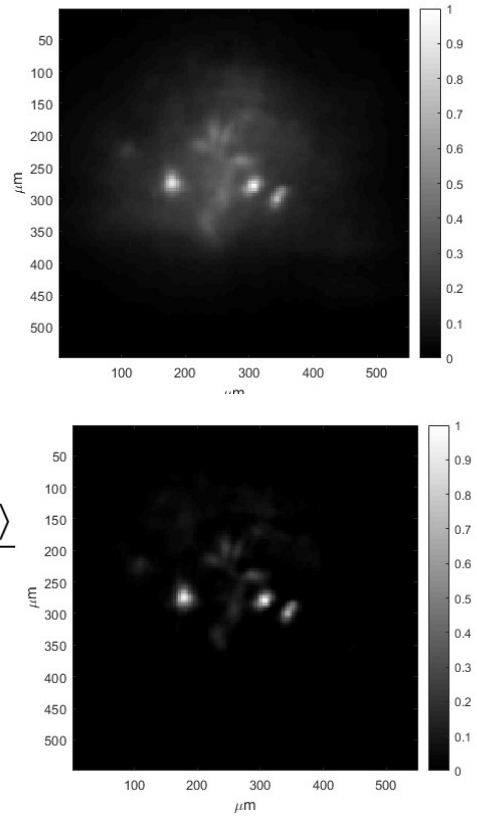

Stacked refocusing

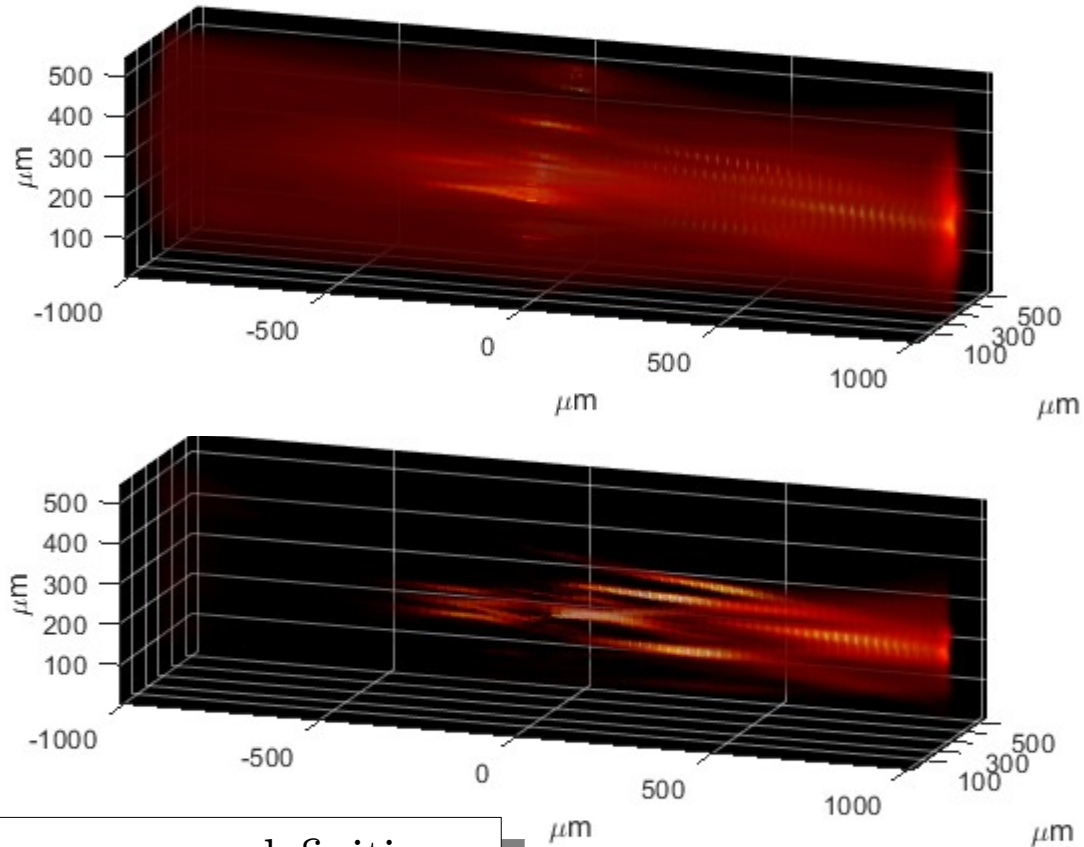

The images Σ contain a background that can be removed by a proper redefinition of the computed correlation function (experimental data: starch in gel).

Seminal ideal (differential ghost imaging) by F. Ferri, D. Magatti, L. A. Lugiato, A. Gatti, PRL 104, 253603 (2010).

3D Reconstruction

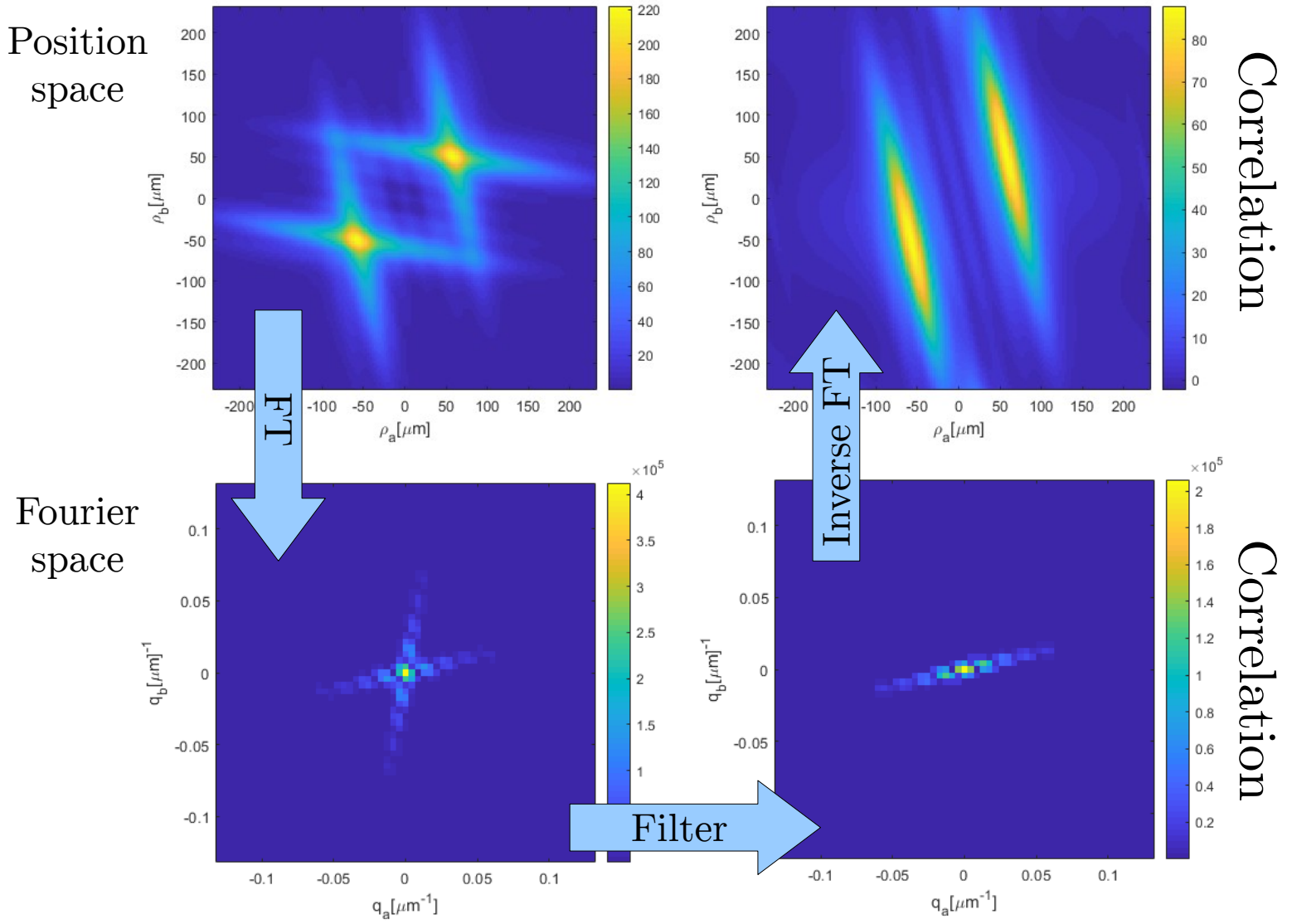

The Fourier transform of the correlation function is concentrated along a direction defined by the distance from the lens.

The choice of the filter determines the specific plane to reconstruct.

Qu3D

Quantum 3D imaging at high speed and high resolution

1. Single-lens plenoptic camera based on a chaotic light source, making 3D imaging at high speed (>10 fps) and high SNR.
2. Ultra-low noise plenoptic device based on entangled photon pairs, enabling 3D imaging of low-absorption samples, at the shot-noise limit or below.

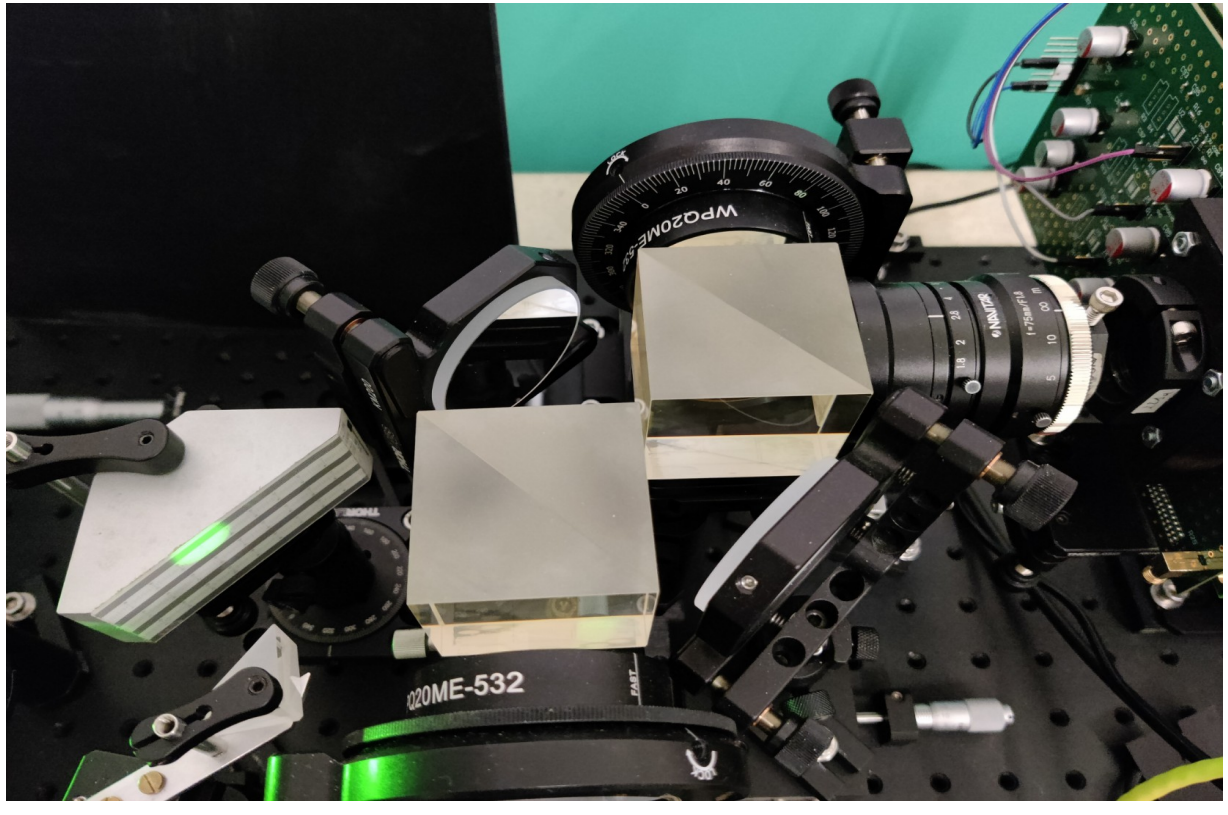

CPI between Arbitrary Planes (AP)

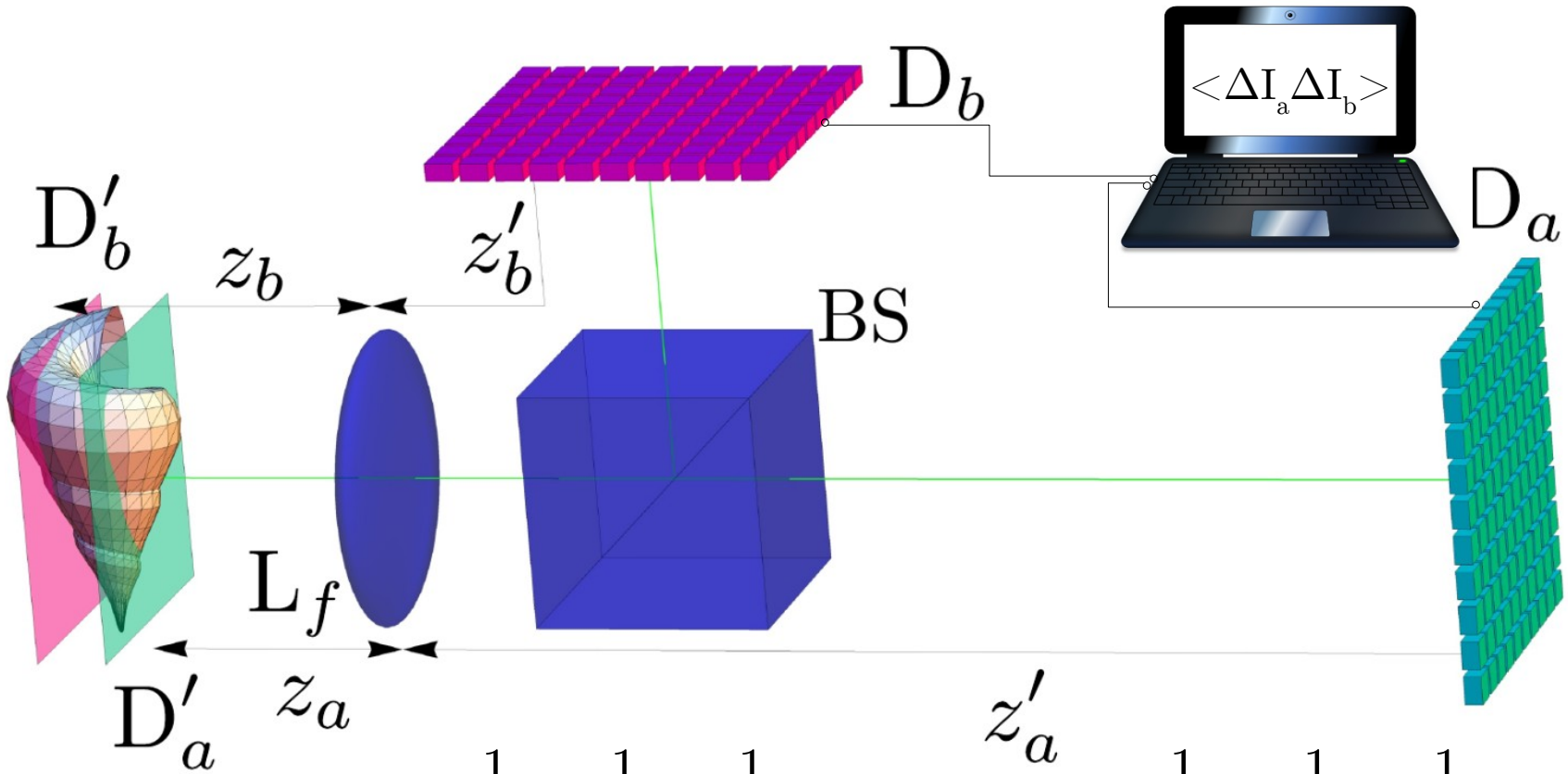

A light crossing both planes D'_a and D'_b, within the 3D scene, is collected by both detectors D_a and D_b, and can thus be reconstructed.

- F. Di Lena, M. D'Angelo, F. V. Pepe, A. Garuccio, brevetto internazionale PCT/IB2019/052351 depositato il 22/03/2019.
- F. Di Lena, G. Massaro, A. Lupo, A. Garuccio, F. V. Pepe, and M. D'Angelo, Optics Express, vol. 28, n. 24, pp. 35857–35868, 2020.

CPI between Arbitrary Planes (AP)

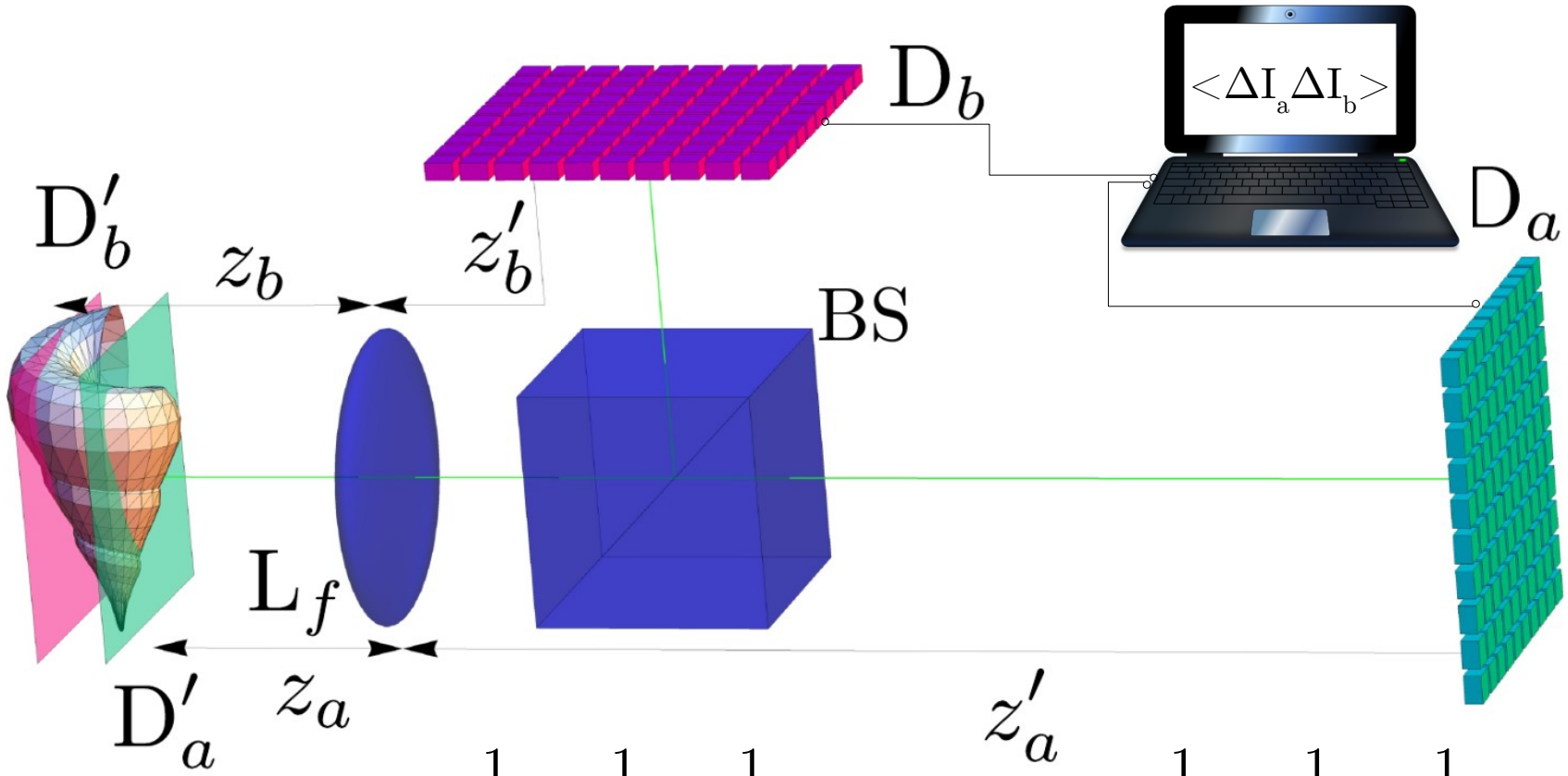

$$\frac{1}{z_b} + \frac{1}{z'_b} = \frac{1}{f} \qquad \frac{1}{z_a} + \frac{1}{z'_a} = \frac{1}{f}$$

Acquired images

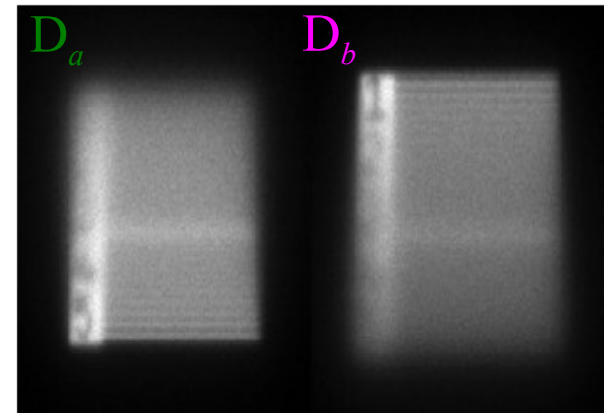

Refocused

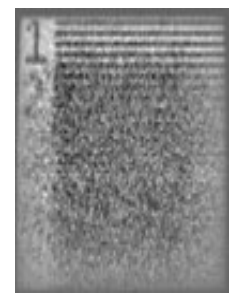

Stacked

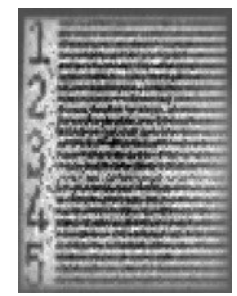

- F. Di Lena, M. D'Angelo, F. V. Pepe, A. Garuccio, brevetto internazionale PCT/IB2019/052351 depositato il 22/03/2019.
- F. Di Lena, G. Massaro, A. Lupo, A. Garuccio, F. V. Pepe, and M. D'Angelo, Optics Express, vol. 28, n. 24, pp. 35857–35868, 2020.

CPI between Arbitrary Planes (AP)

Advantages:

1. Further DOF enhancement with respect previous CPI.
2. No image of the focusing element.
3. One more plane with diffraction-limited resolution.

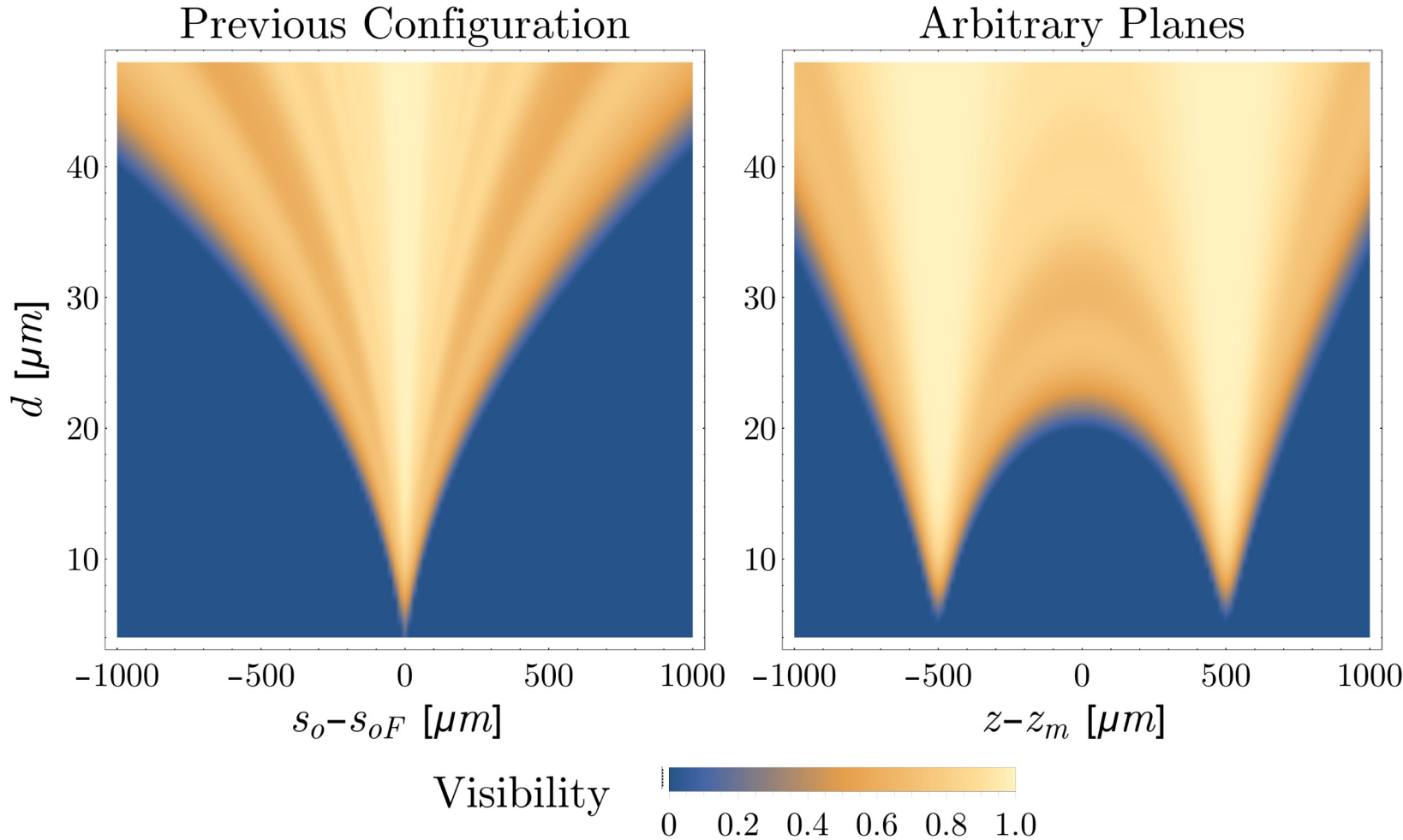

- F. Di Lena, M. D'Angelo, F. V. Pepe, A. Garuccio, brevetto internazionale PCT/IB2019/052351 depositato il 22/03/2019.
- F. Di Lena, G. Massaro, A. Lupo, A. Garuccio, F. V. Pepe, and M. D'Angelo, Optics Express, vol. 28, n. 24, pp. 35857–35868, 2020.

Single-lens correlation plenoptic camera

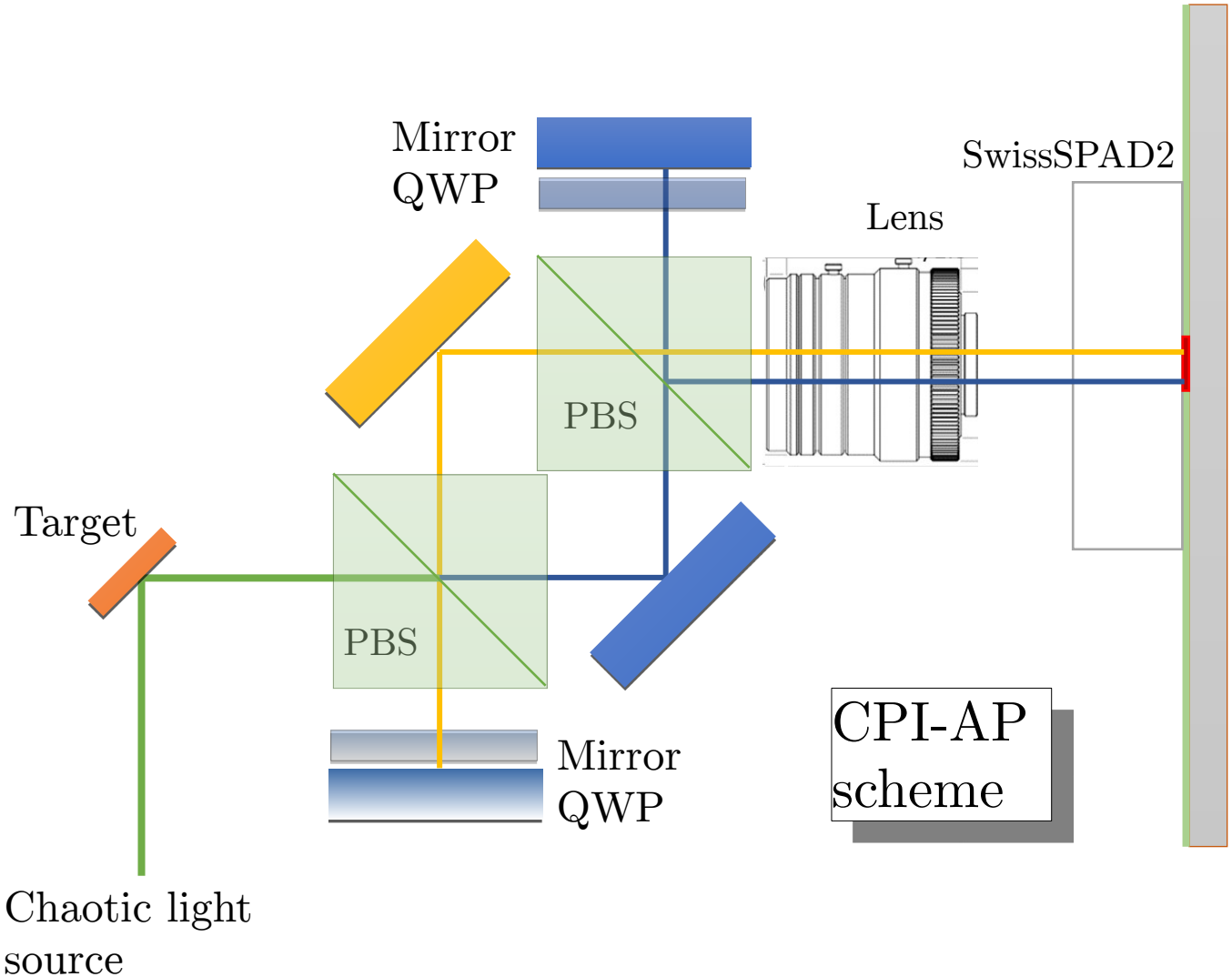

Single-lens correlation plenoptic camera

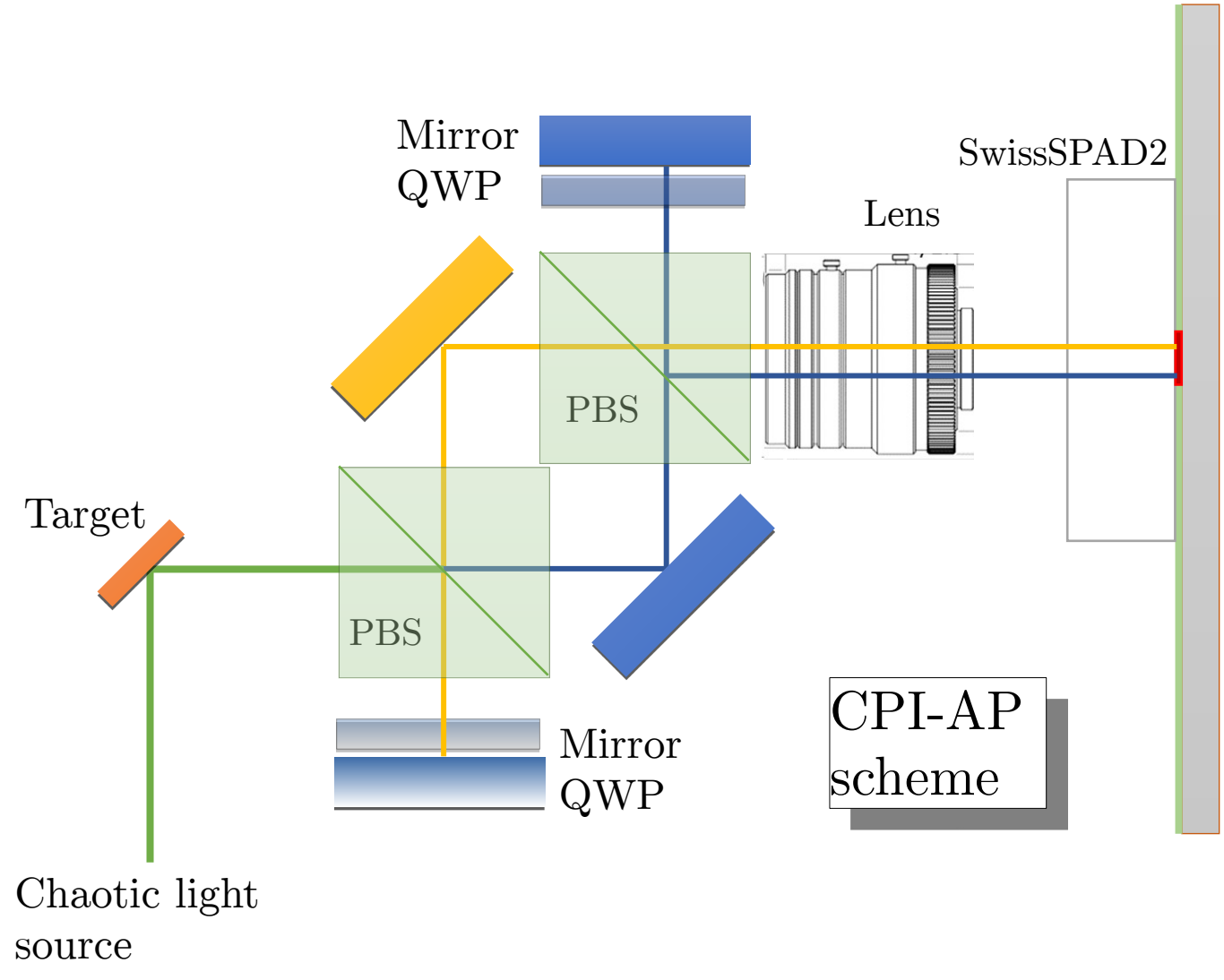

Very first CPI between AP

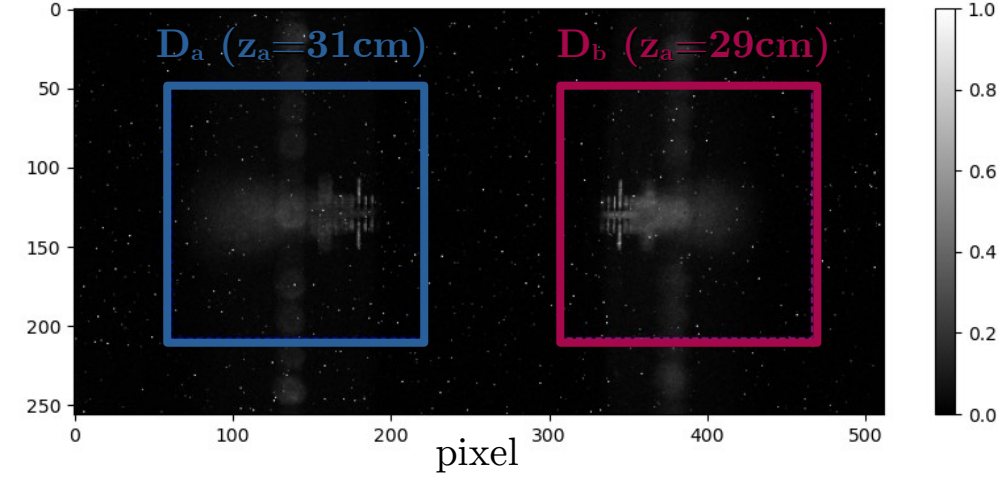

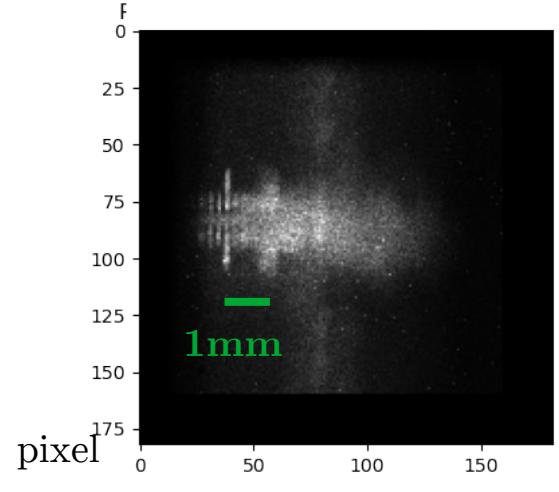

Refocus at
z = 29.0 cm

Single-lens correlation plenoptic camera

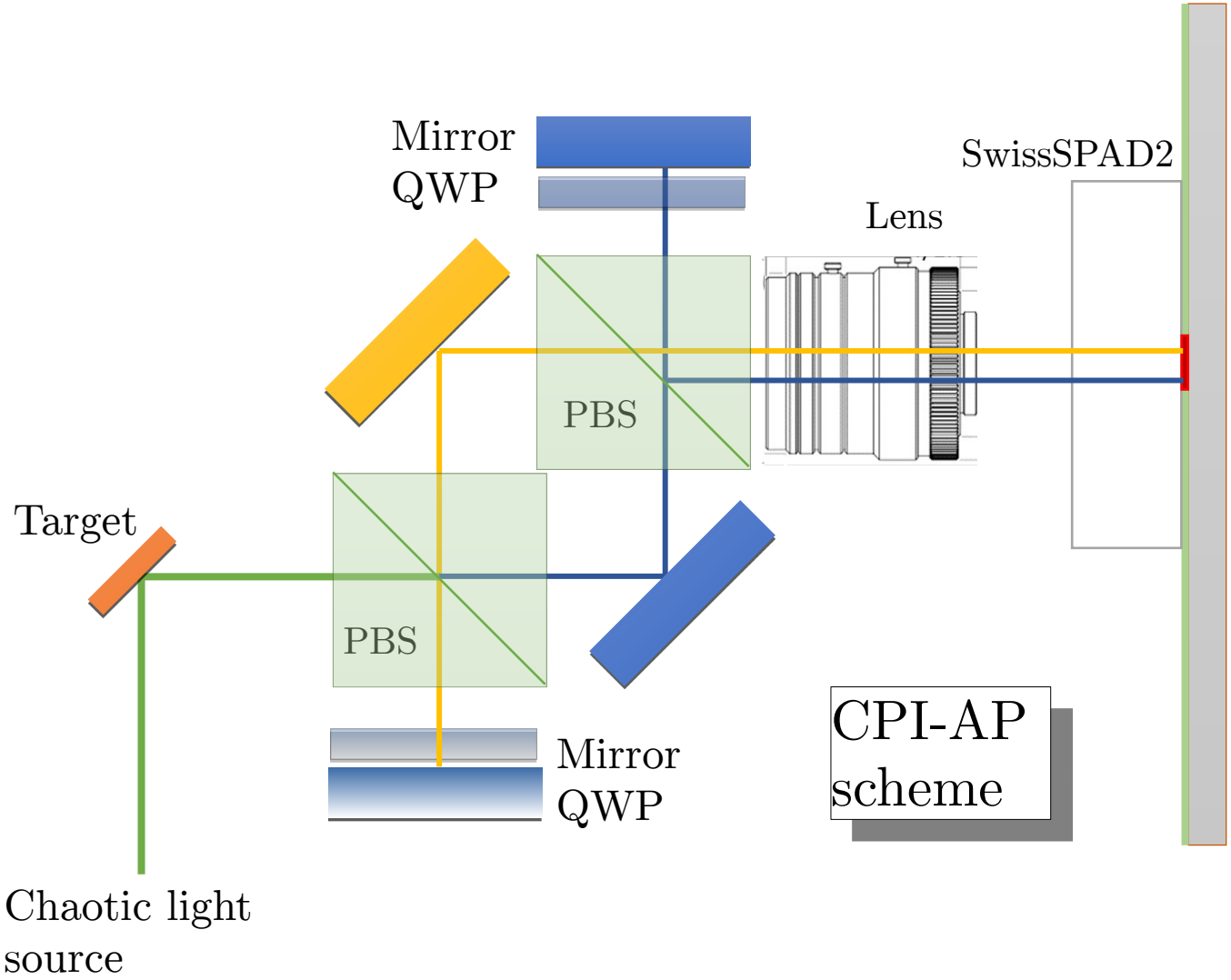

Very first CPI between AP

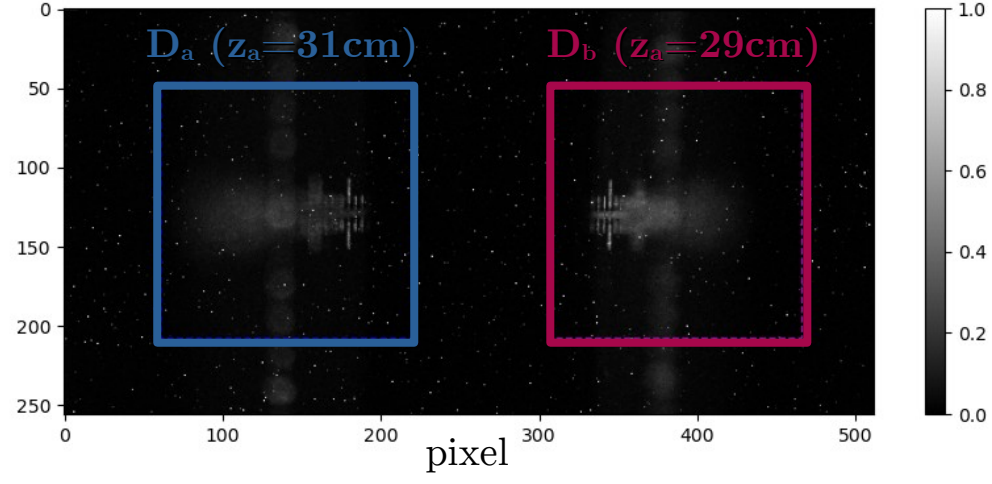

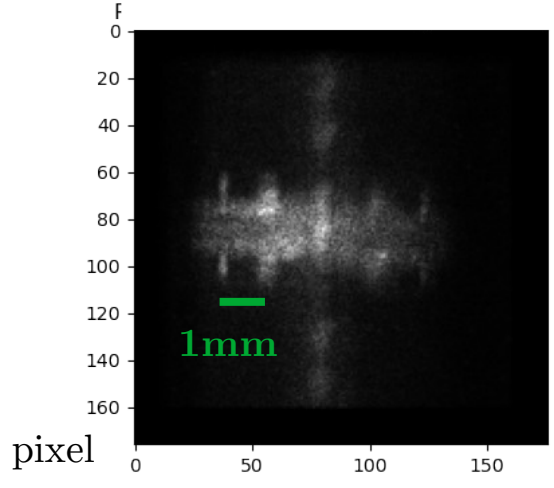

Refocus at
z = 29.5 cm

Single-lens correlation plenoptic camera

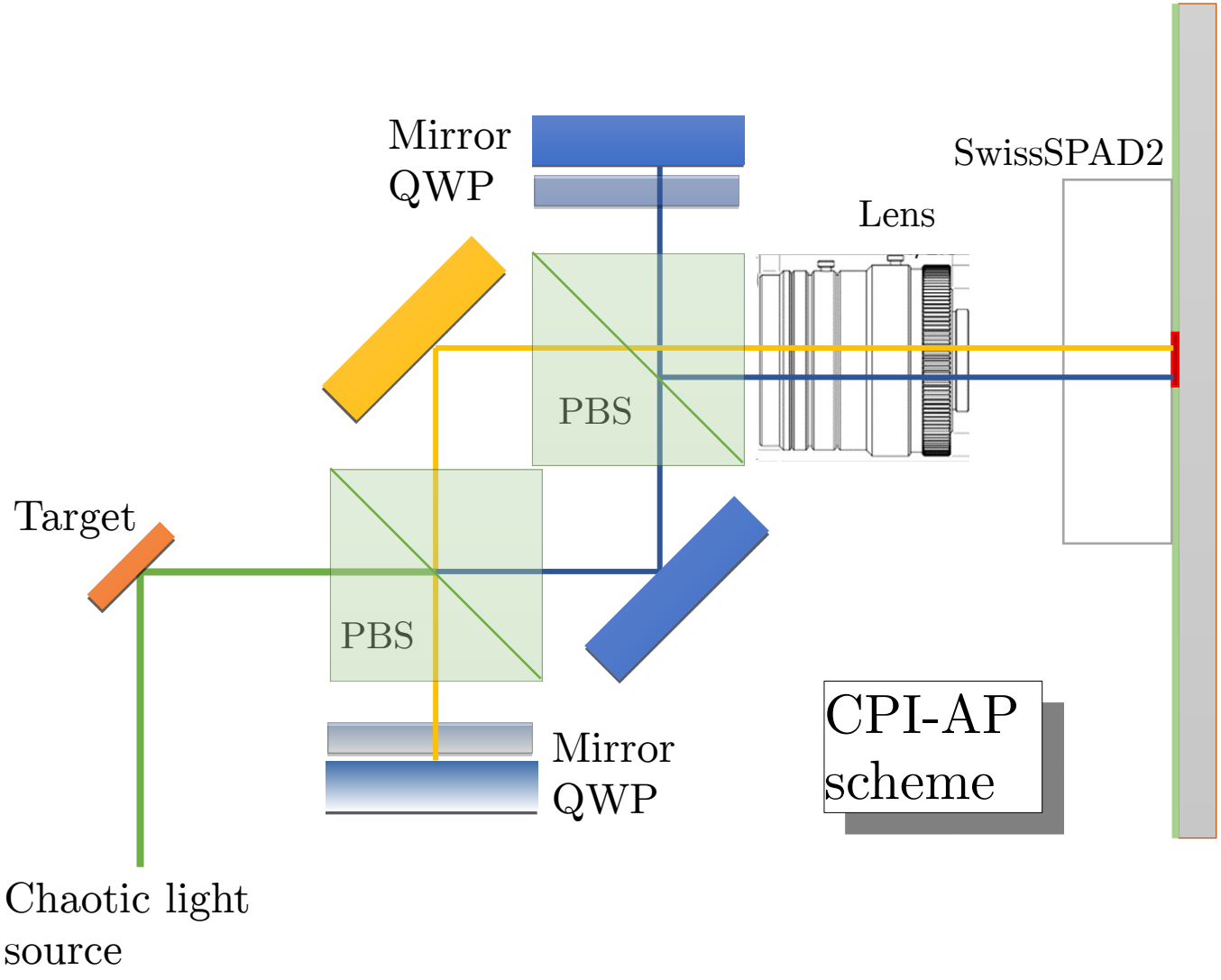

Very first CPI between AP

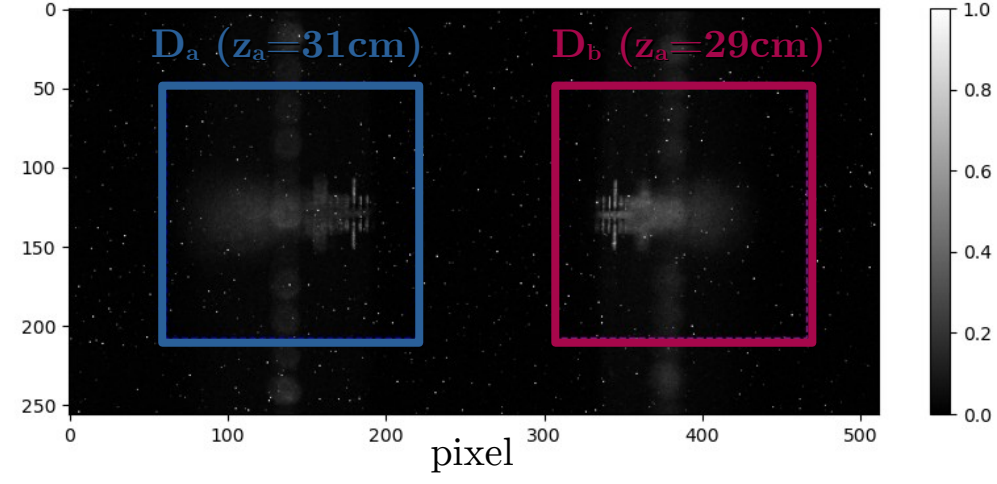

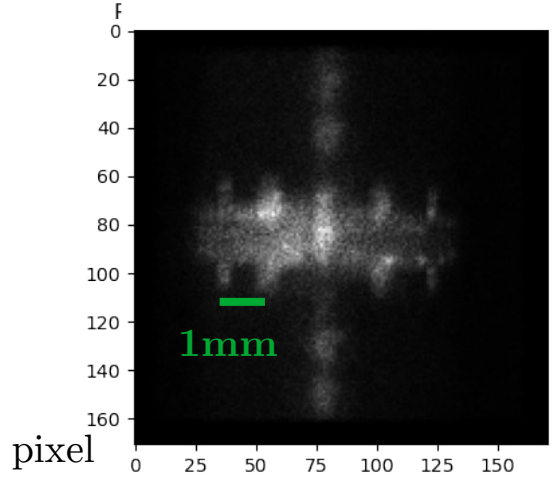

Refocus at
z = 30.0 cm

Single-lens correlation plenoptic camera

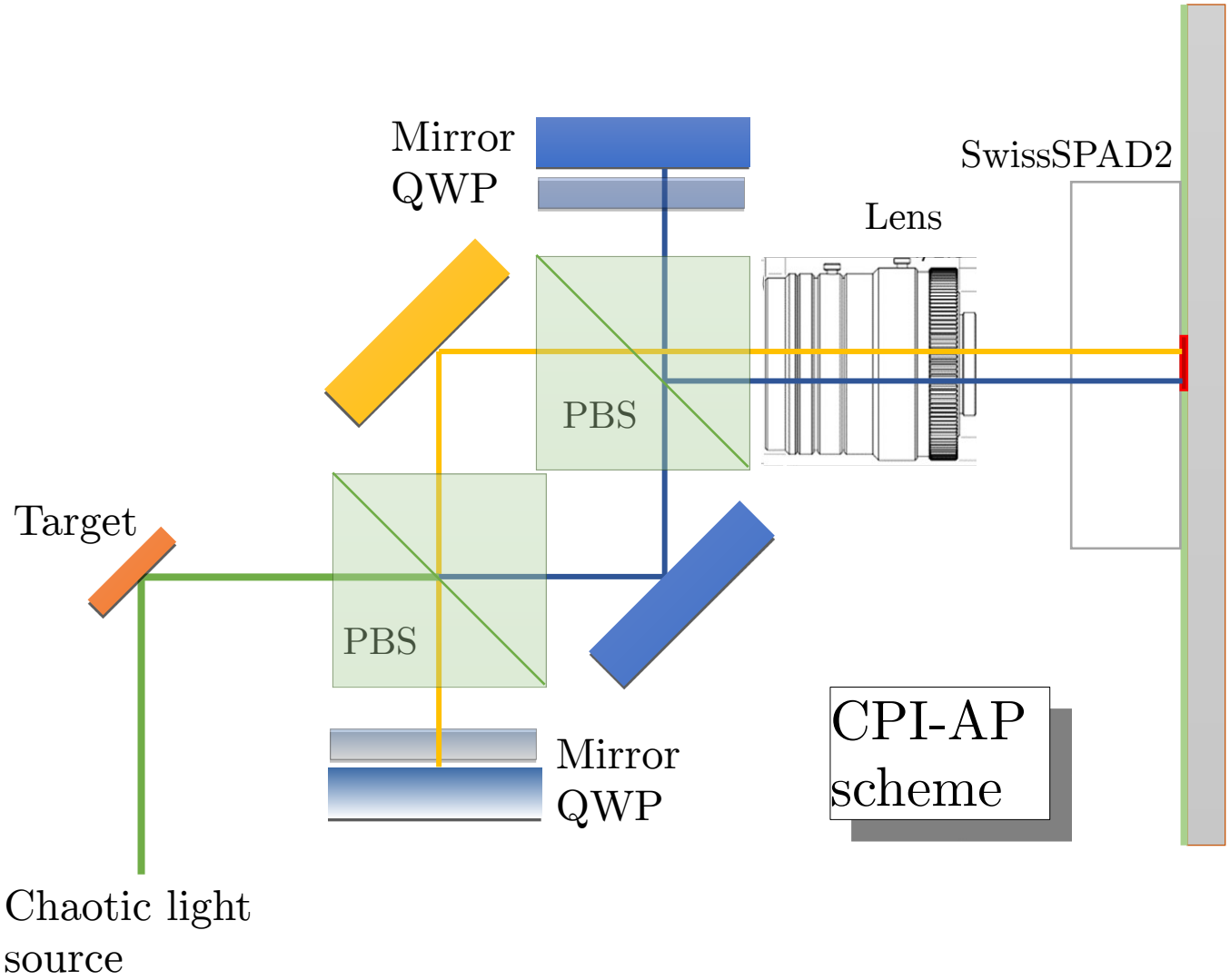

Very first CPI between AP

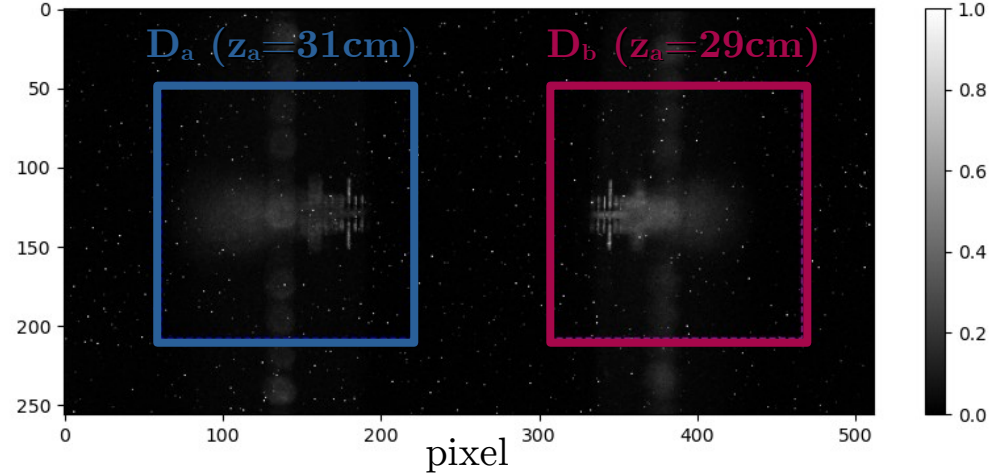

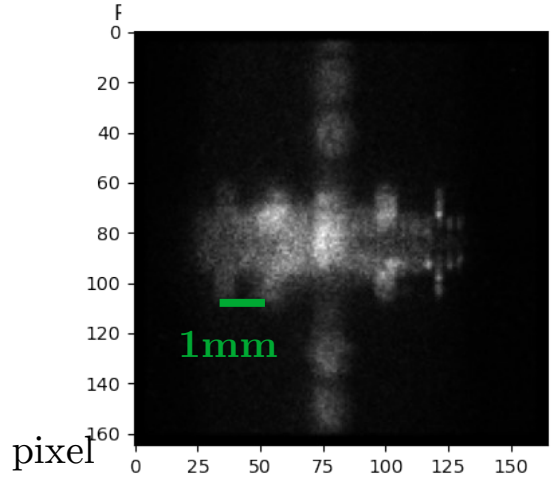

Refocus at
z = 30.5 cm

Single-lens correlation plenoptic camera

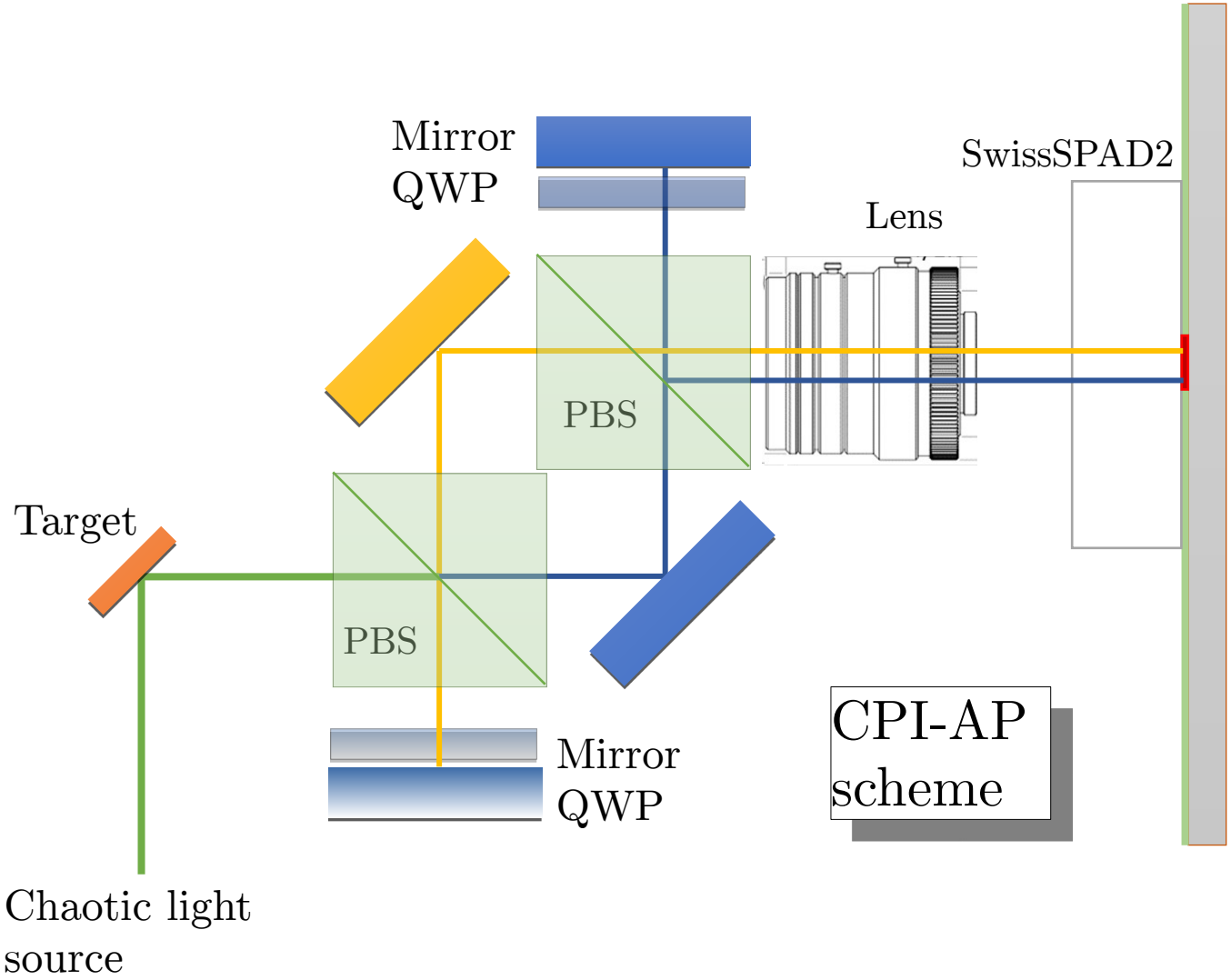

Very first CPI between AP

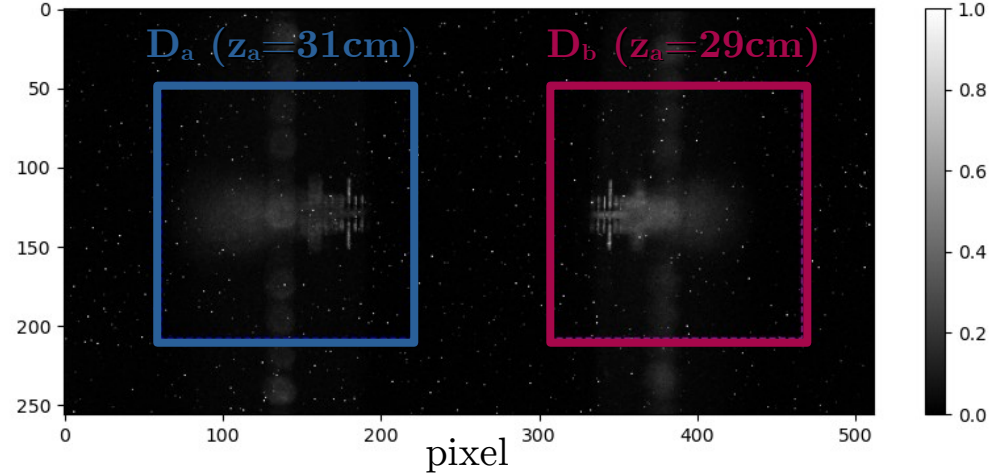

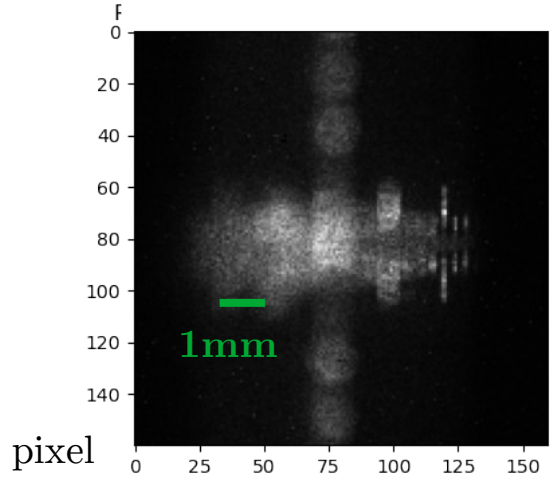

Refocus at
z = 31.0 cm

Toward ultra-fast CPI

- Hardware
  - Ultra-fast SPAD array (École Polytechnique Fédérale de Lausanne).
  - Parallel computing with GPU (Planetek).
- Software
  - Compressive sensing (Planetek)
  - Quantum tomography reconstruction (Palacky University Olomouc).
- Quantum Fisher information (Palacky University Olomouc).

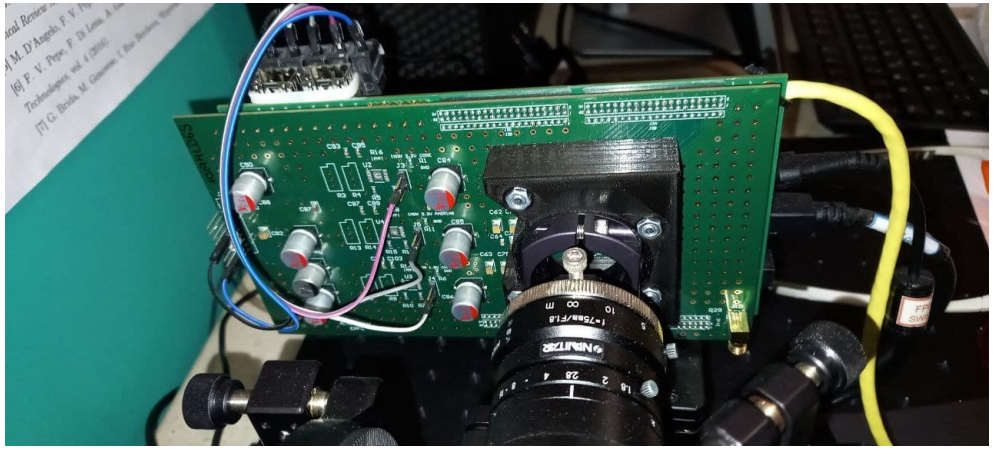

EPFL SwissSPAD (larger available SPAD array):

- Resolution = 512×512 pixel
- Pixel size = 16.38 μm
- Speed = 10^5 frame/s
- Min. exposure = 10 ns
- QE ≈ 0.45

CPI-AP with entangled photons

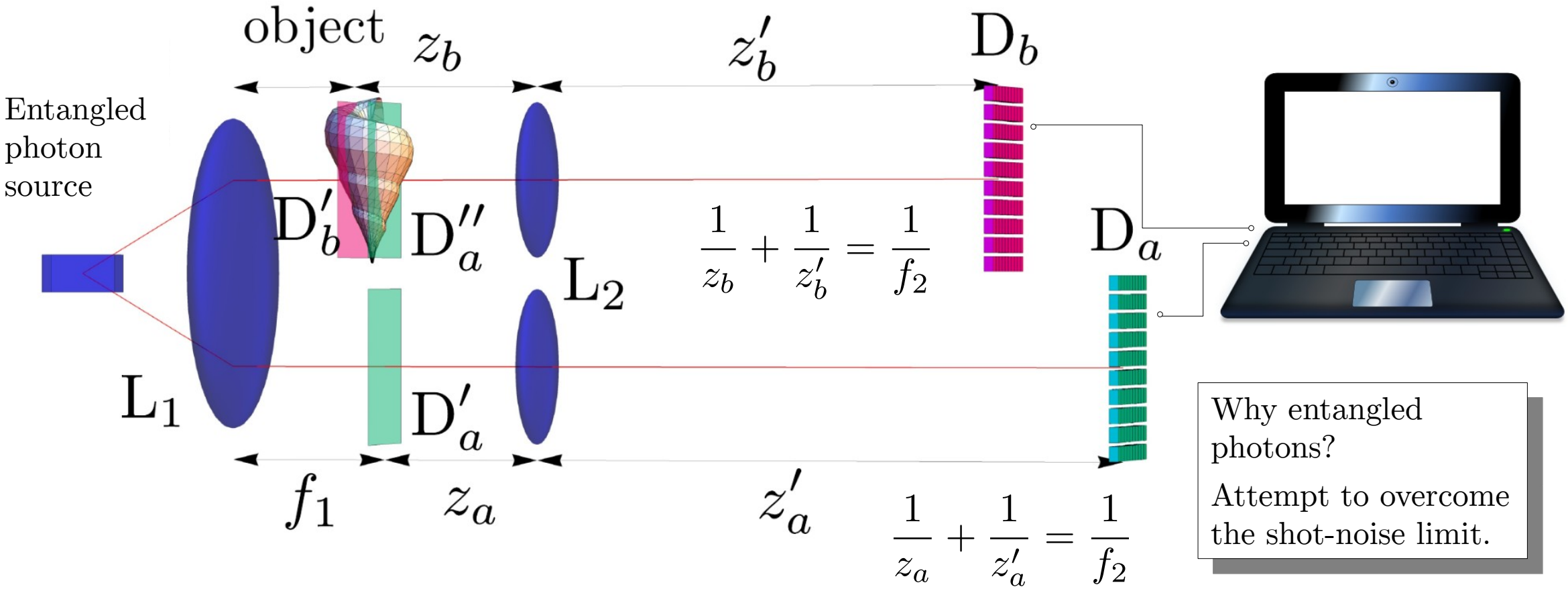

Why entangled photons?

Attempt to overcome the shot-noise limit.

- F. Di Lena, M. D'Angelo, F. V. Pepe, A. Garuccio, brevetto internazionale PCT/IB2019/052351 depositato il 22/03/2019.
- F. Di Lena, G. Massaro, A. Lupo, A. Garuccio, F. V. Pepe, and M. D'Angelo, Optics Express, vol. 28, n. 24, pp. 35857–35868, 2020.

TOPMIRCO

TOward the Prototype of a Correlation Plenoptic MICROscope

Goals:

- Technical development and valorization of the international pantent on CPM (n. 102018000007857, 2018, PICS).

From TRL* 3 to TRL 6, for the observation of biological and medical samples.

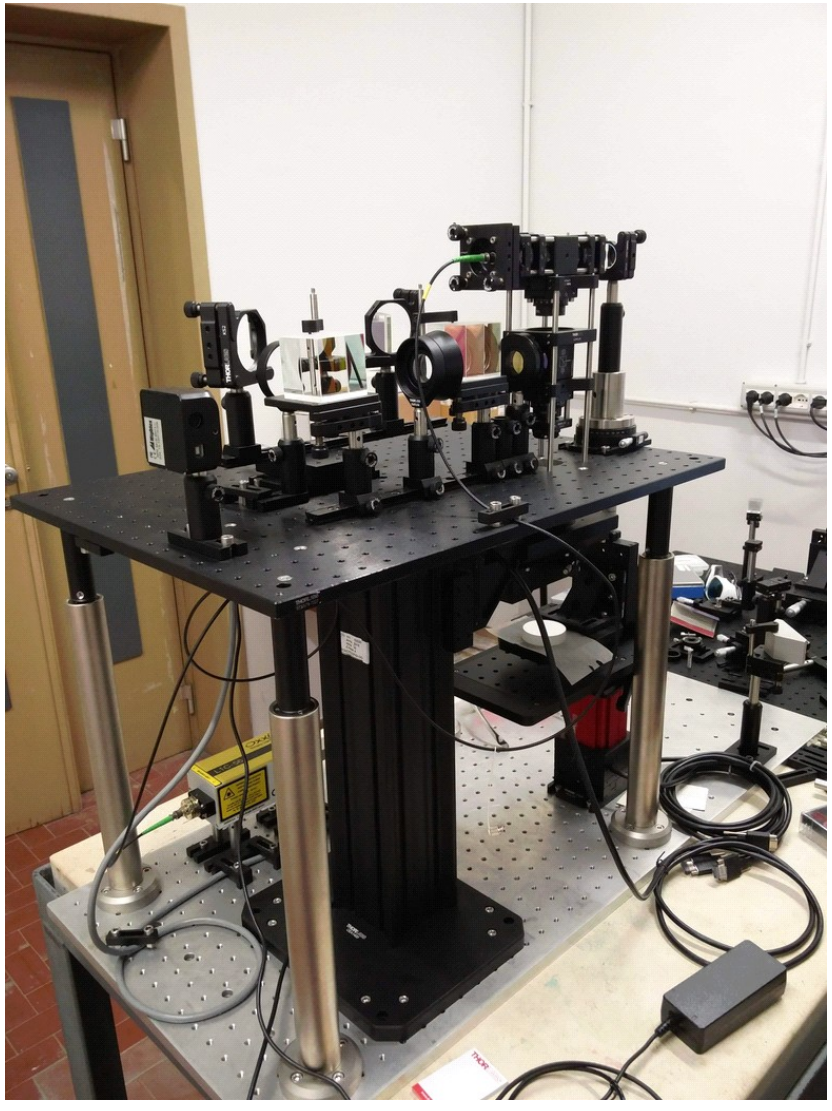

* Technology Readiness Level

CPM prototype

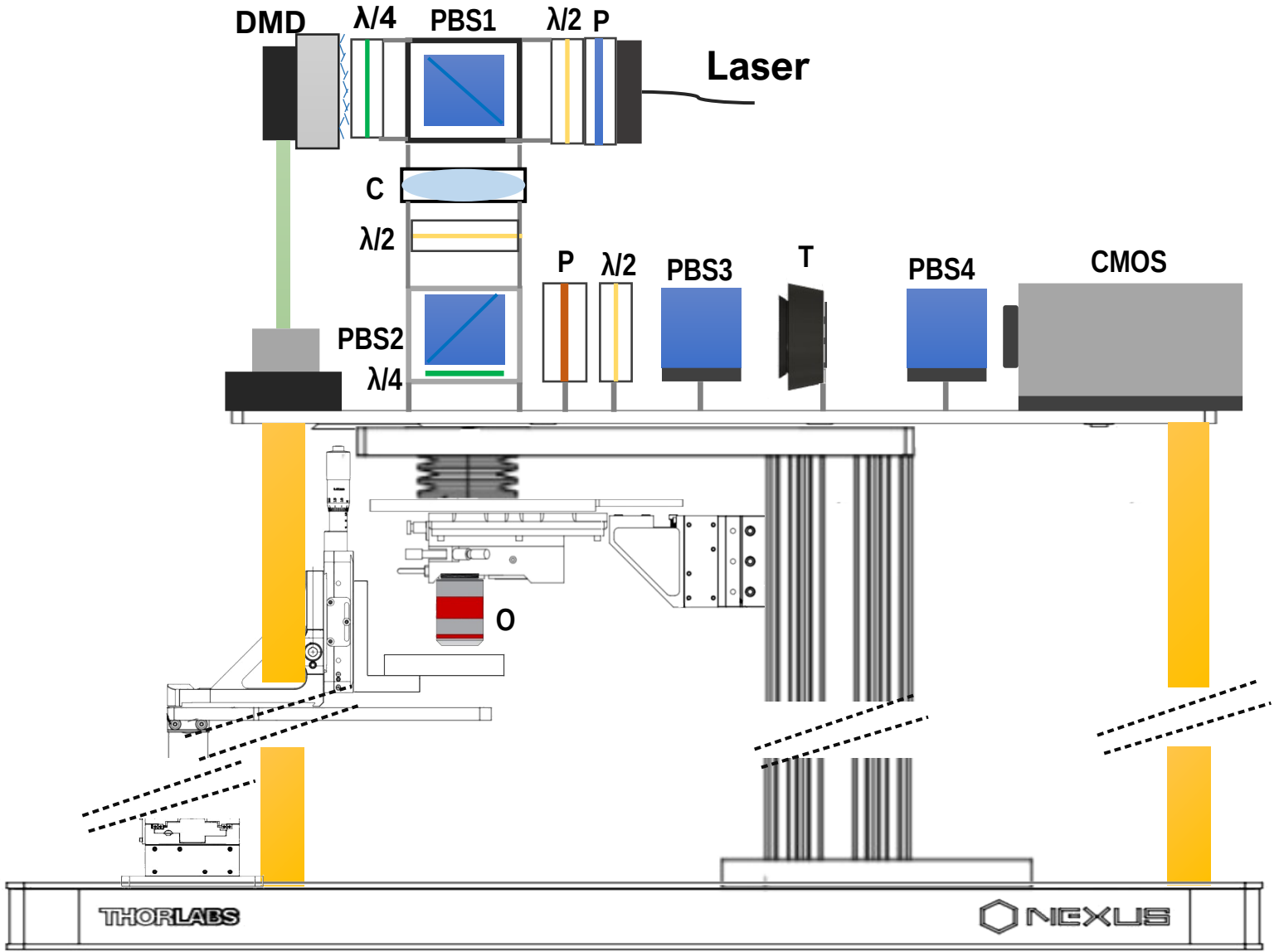

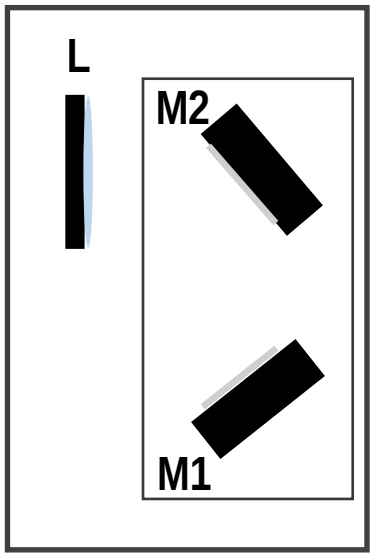

Conversion to arbitrary planes is under construction.

In summary...

Results

- ✔ Our contribution to quantum 2.0 → CPI
- ✔ Correlation plenoptic microscopy → prototype for scanning-free 3D imaging.
- ✔ CPI between planes → towad novel imaging devices (EU project).

Papers, patents & projects

- ✔ 2 PRL
- ✔ 5 patens (one awarded)
- ✔ 3 ongoing INFN projects.
- ✔ 1 UniBA project

Research group

- Students:
  - Davide Giannella
  - Gianlorenzo Massaro
- Post-docs:
  - Francesco Di Lena
  - Sergeii Vasiukov
- Reaserchers:
  - Francesco Pepe
  - Francesco Scattarella
- Permament:
  - Milena D'Angelo

Thanks for your attention!

Appendix

Tomography from Palacky University Olomouc

$$\bar{n}_j = \bar{n}_0 e^{-\int \mu(x,y,z) ds_j}$$

From a CPI measurement we can estimate the absorption function μ(x,y,x) by the maximum likelihood method.

Refocusing

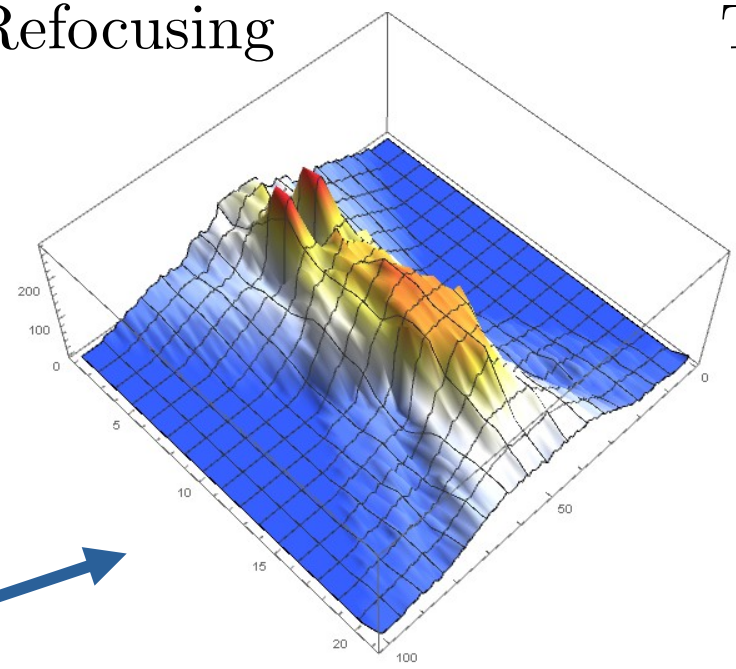

Tomography

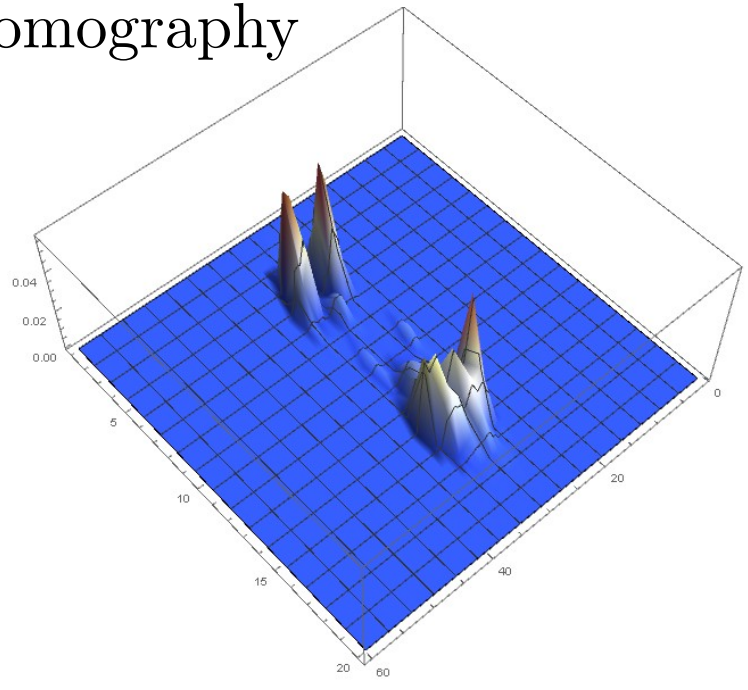

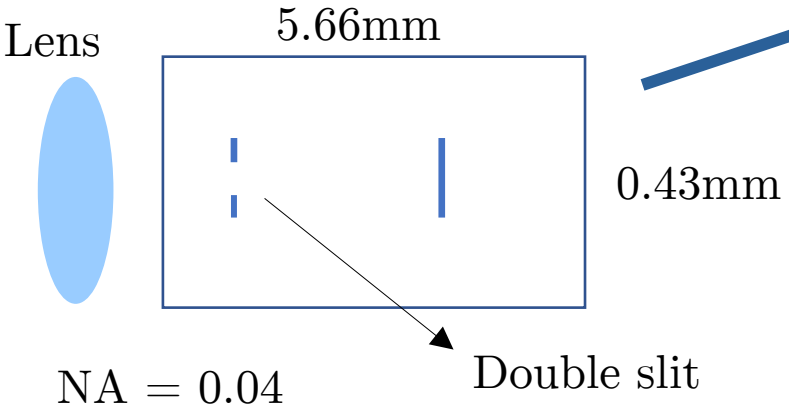

NA = 0.04

- As opposed to refocus, by a tomography is it possible to remove the blurred area.
- Larger NA is required of getting reconstruction of more complex 3D samples.

Appendix

CPI working principle

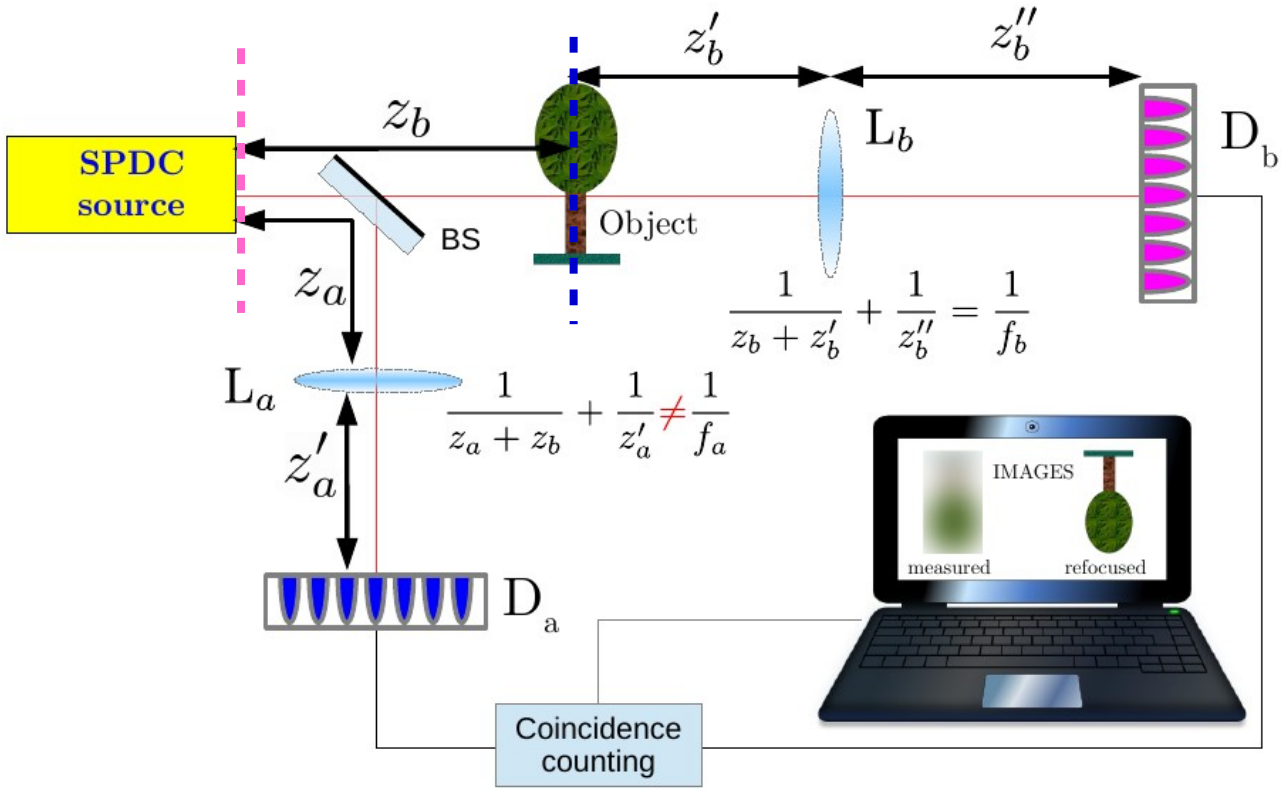

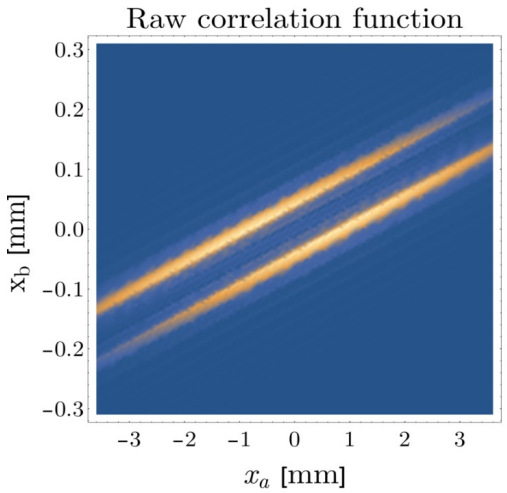

Object is a double slit

$$G^{(2)}(\rho_a, \rho_b; t_a, t_b) =$$
$$< E_a^{(-)}(\rho_a, t_a) E_b^{(-)}(\rho_b, t_b) E_a^{(+)}(\rho_a, t_a) E_b^{(+)}(\rho_b, t_b) >$$

$E_j \rightarrow$ Field at the detectors

F. V. Pepe, F. Di Lena, A. Garuccio, G. Scarcelli, and M. D'Angelo, Technologies, vol. 4, no. 2, p. 17, 2016

Appendix

CPI working principle

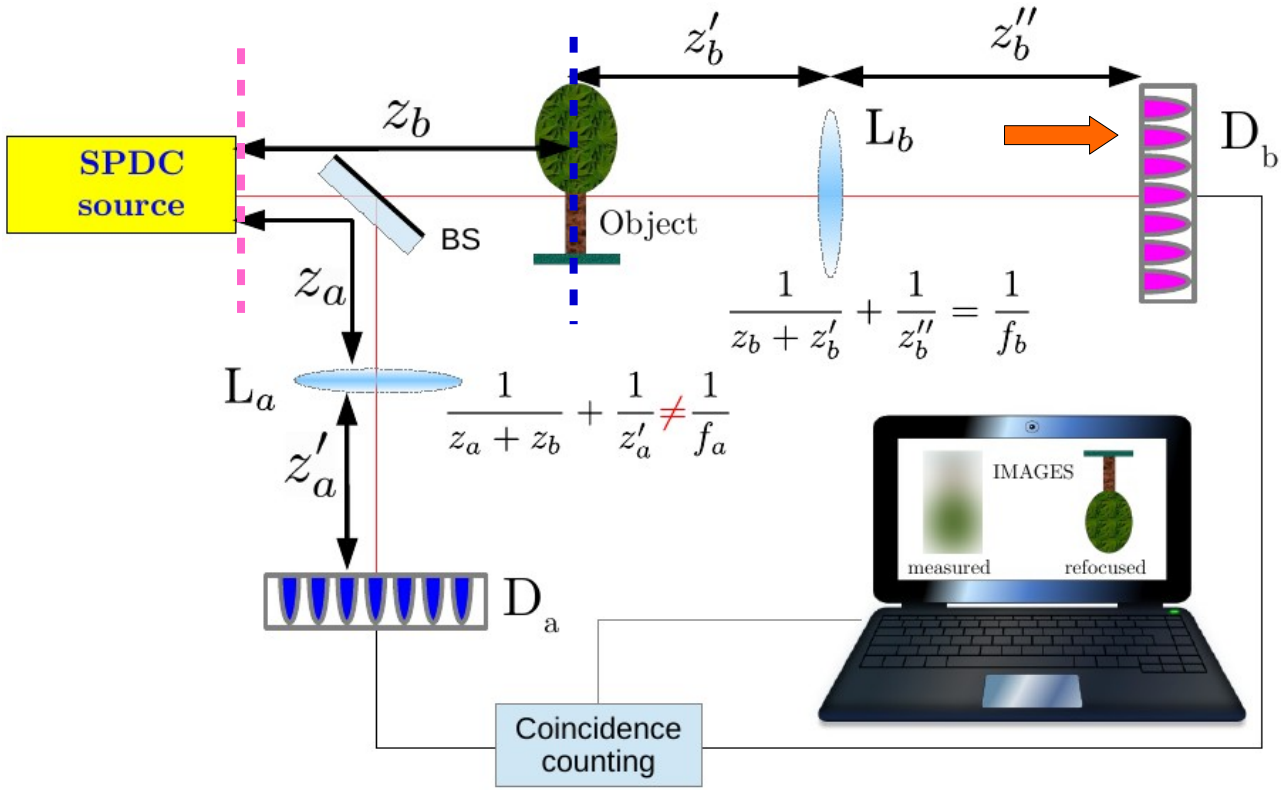

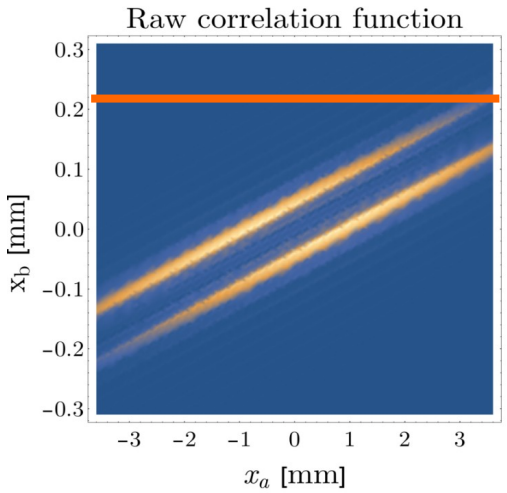

$$G^{(2)}(\rho_a, \rho_b; t_a, t_b) =$$
$$< E_a^{(-)}(\rho_a, t_a) E_b^{(-)}(\rho_b, t_b) E_a^{(+)}(\rho_a, t_a) E_b^{(+)}(\rho_b, t_b) >$$

$E_j \rightarrow$ Field at the detectors

- F. V. Pepe, F. Di Lena, A. Garuccio, G. Scarcelli, and M. D'Angelo, Technologies, vol. 4, no. 2, p. 17, 2016

Appendix

CPI working principle

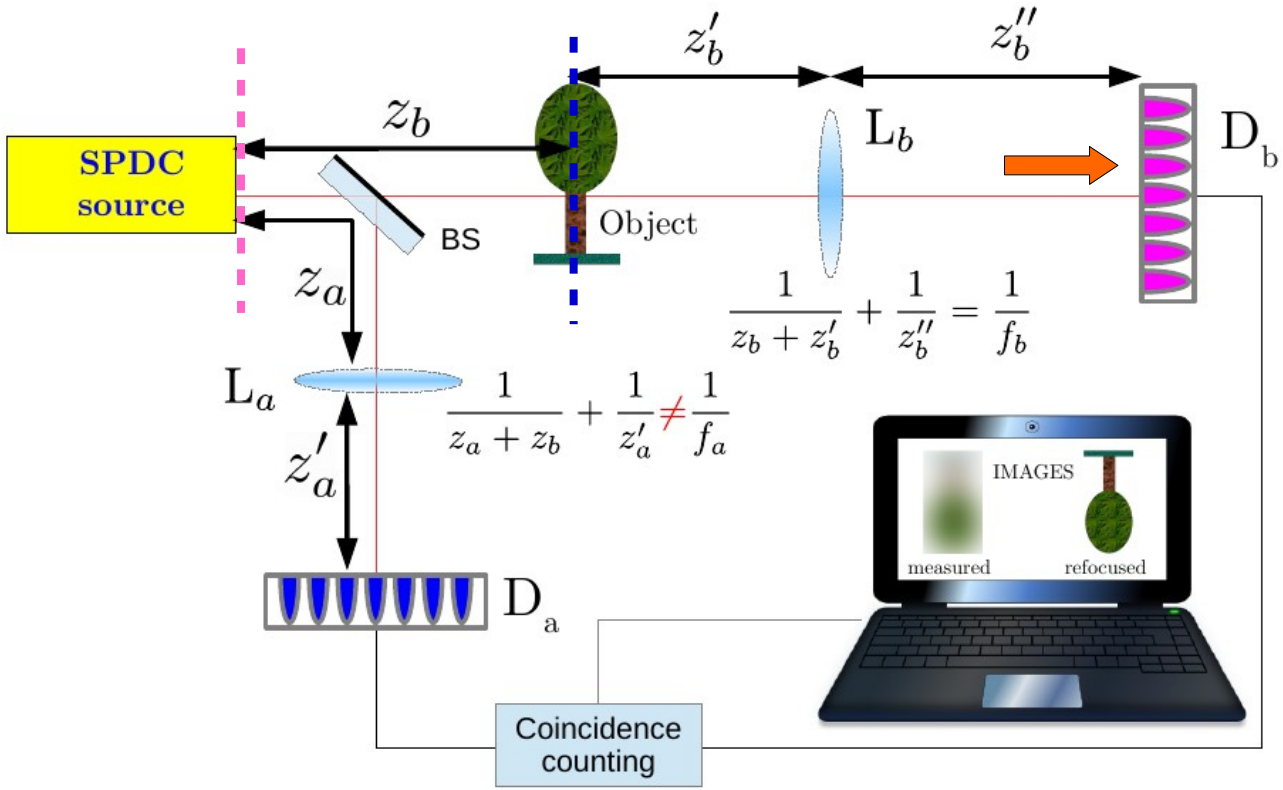

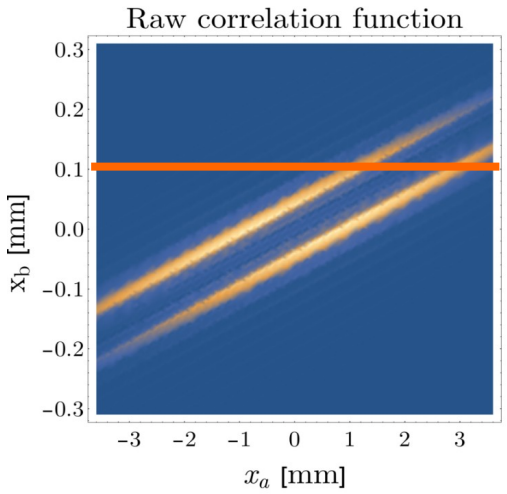

$$G^{(2)}(\rho_a, \rho_b; t_a, t_b) =$$
$$< E_a^{(-)}(\rho_a, t_a) E_b^{(-)}(\rho_b, t_b) E_a^{(+)}(\rho_a, t_a) E_b^{(+)}(\rho_b, t_b) >$$

$E_j \rightarrow$ Field at the detectors

- F. V. Pepe, F. Di Lena, A. Garuccio, G. Scarcelli, and M. D'Angelo, Technologies, vol. 4, no. 2, p. 17, 2016

Appendix

CPI working principle

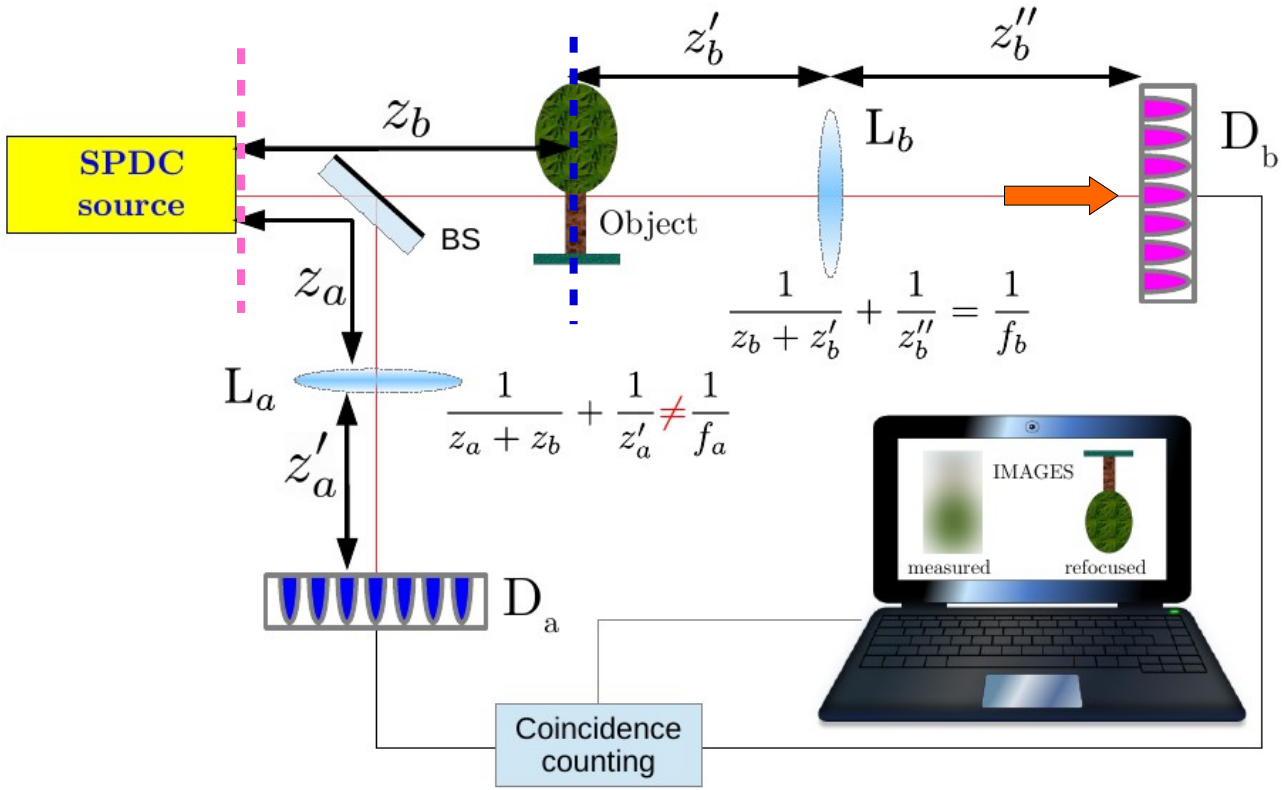

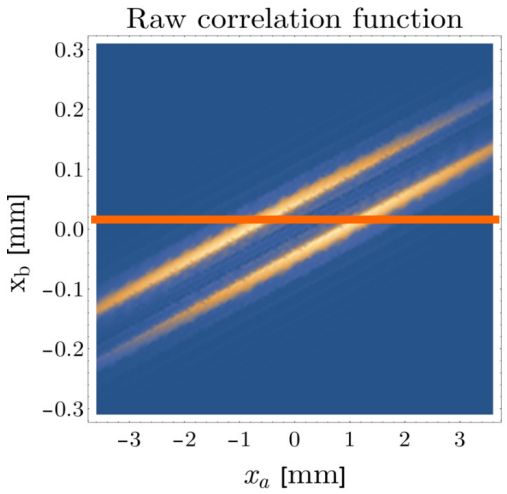

$$G^{(2)}(\rho_a, \rho_b; t_a, t_b) =$$
$$< E_a^{(-)}(\rho_a, t_a) E_b^{(-)}(\rho_b, t_b) E_a^{(+)}(\rho_a, t_a) E_b^{(+)}(\rho_b, t_b) >$$

$E_j \rightarrow$ Field at the detectors

- F. V. Pepe, F. Di Lena, A. Garuccio, G. Scarcelli, and M. D'Angelo, Technologies, vol. 4, no. 2, p. 17, 2016

Appendix

CPI working principle

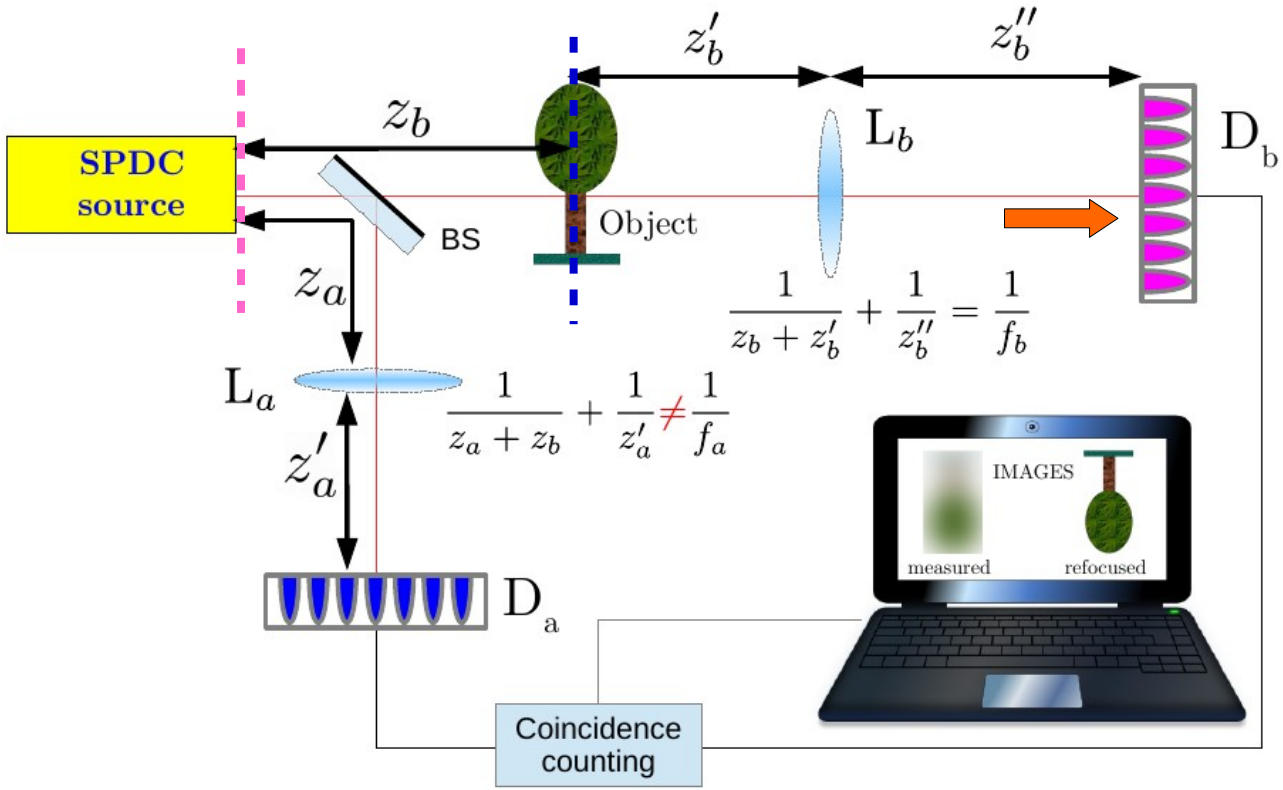

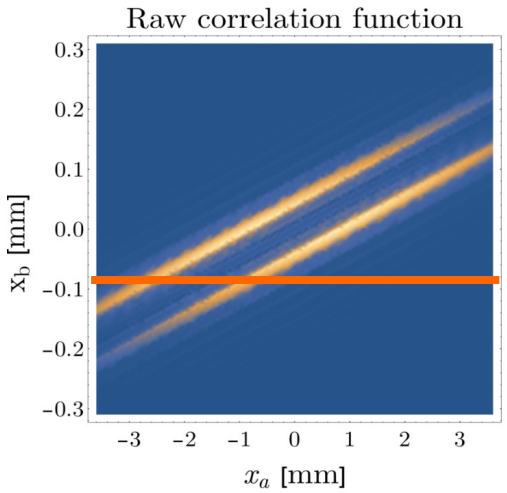

$$G^{(2)}(\rho_a, \rho_b; t_a, t_b) =$$
$$< E_a^{(-)}(\rho_a, t_a) E_b^{(-)}(\rho_b, t_b) E_a^{(+)}(\rho_a, t_a) E_b^{(+)}(\rho_b, t_b) >$$

$E_j \rightarrow$ Field at the detectors

- F. V. Pepe, F. Di Lena, A. Garuccio, G. Scarcelli, and M. D'Angelo, Technologies, vol. 4, no. 2, p. 17, 2016

Appendix

CPI working principle

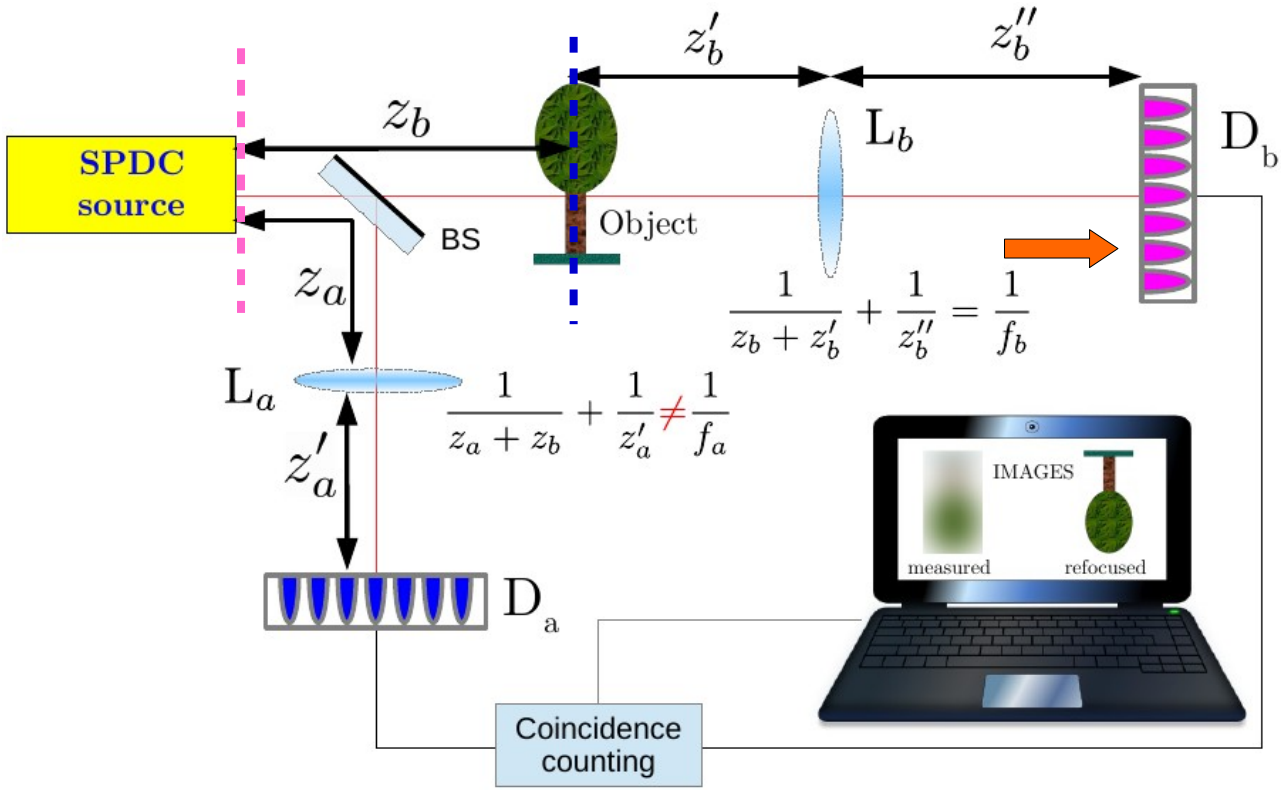

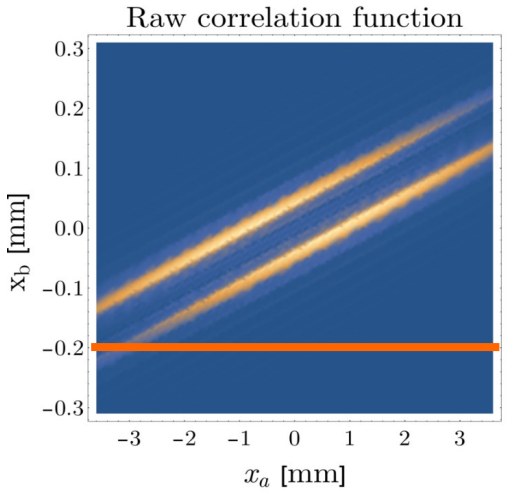

$$G^{(2)}(\rho_a, \rho_b; t_a, t_b) =$$
$$< E_a^{(-)}(\rho_a, t_a) E_b^{(-)}(\rho_b, t_b) E_a^{(+)}(\rho_a, t_a) E_b^{(+)}(\rho_b, t_b) >$$

$E_j \rightarrow$ Field at the detectors

- F. V. Pepe, F. Di Lena, A. Garuccio, G. Scarcelli, and M. D'Angelo, Technologies, vol. 4, no. 2, p. 17, 2016

Appendix

CPI working principle

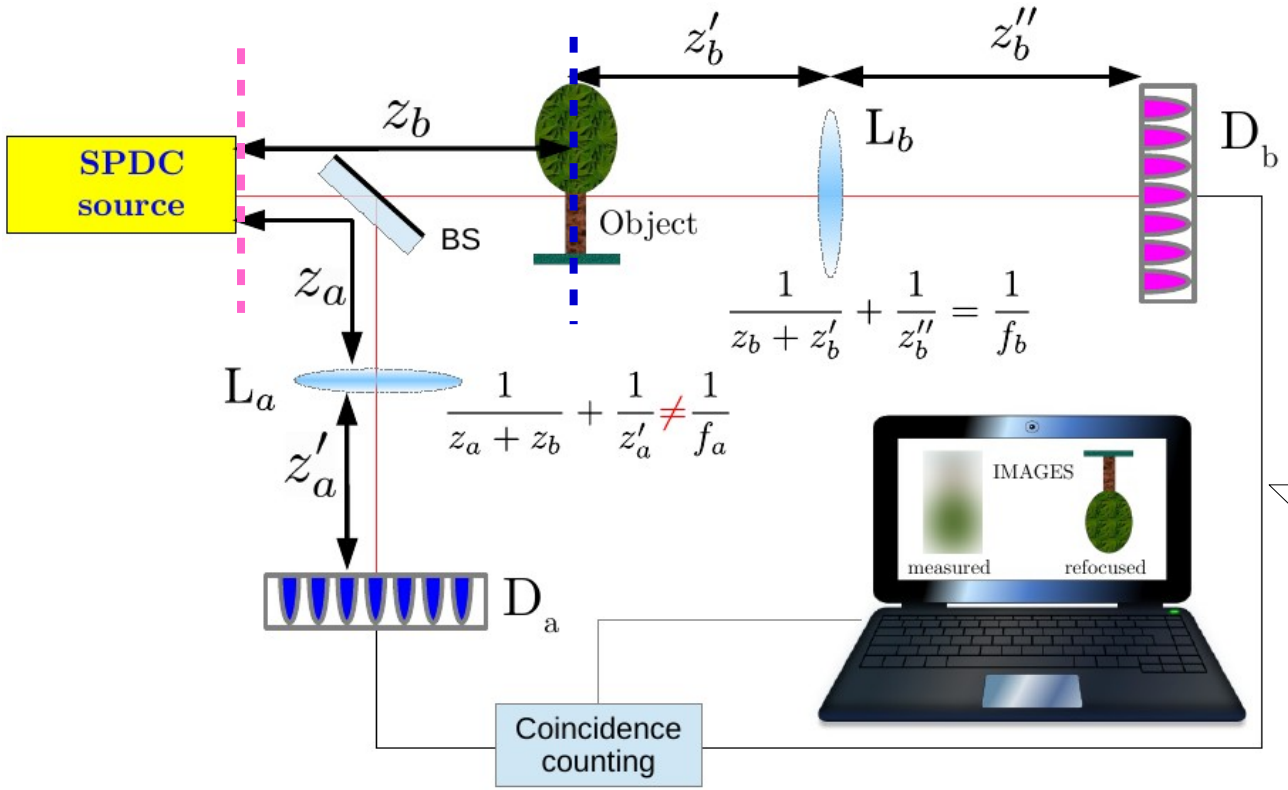

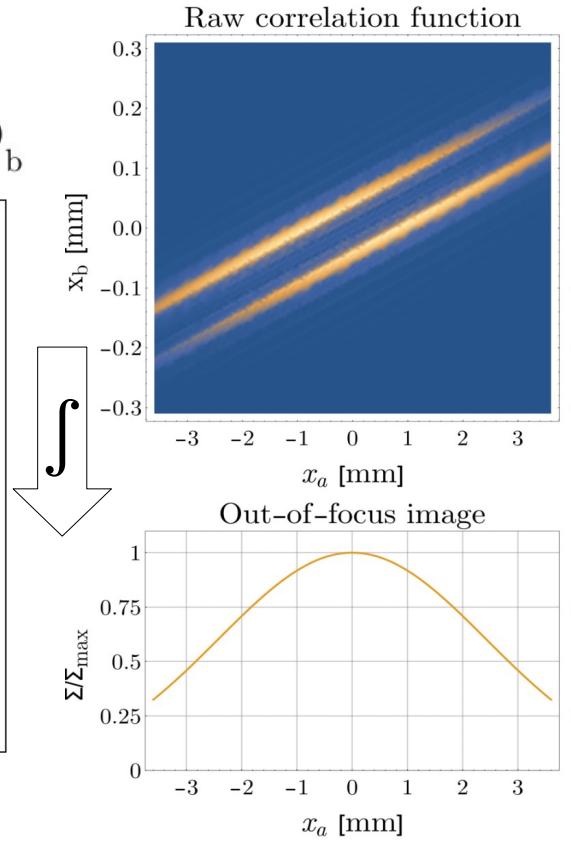

$$G^{(2)}(\rho_a, \rho_b; t_a, t_b) =$$
$$< E_a^{(-)}(\rho_a, t_a) E_b^{(-)}(\rho_b, t_b) E_a^{(+)}(\rho_a, t_a) E_b^{(+)}(\rho_b, t_b) >$$

$E_j \rightarrow$ Field at the detectors

- F. V. Pepe, F. Di Lena, A. Garuccio, G. Scarcelli, and M. D'Angelo, Technologies, vol. 4, no. 2, p. 17, 2016

Appendix

CPI working principle

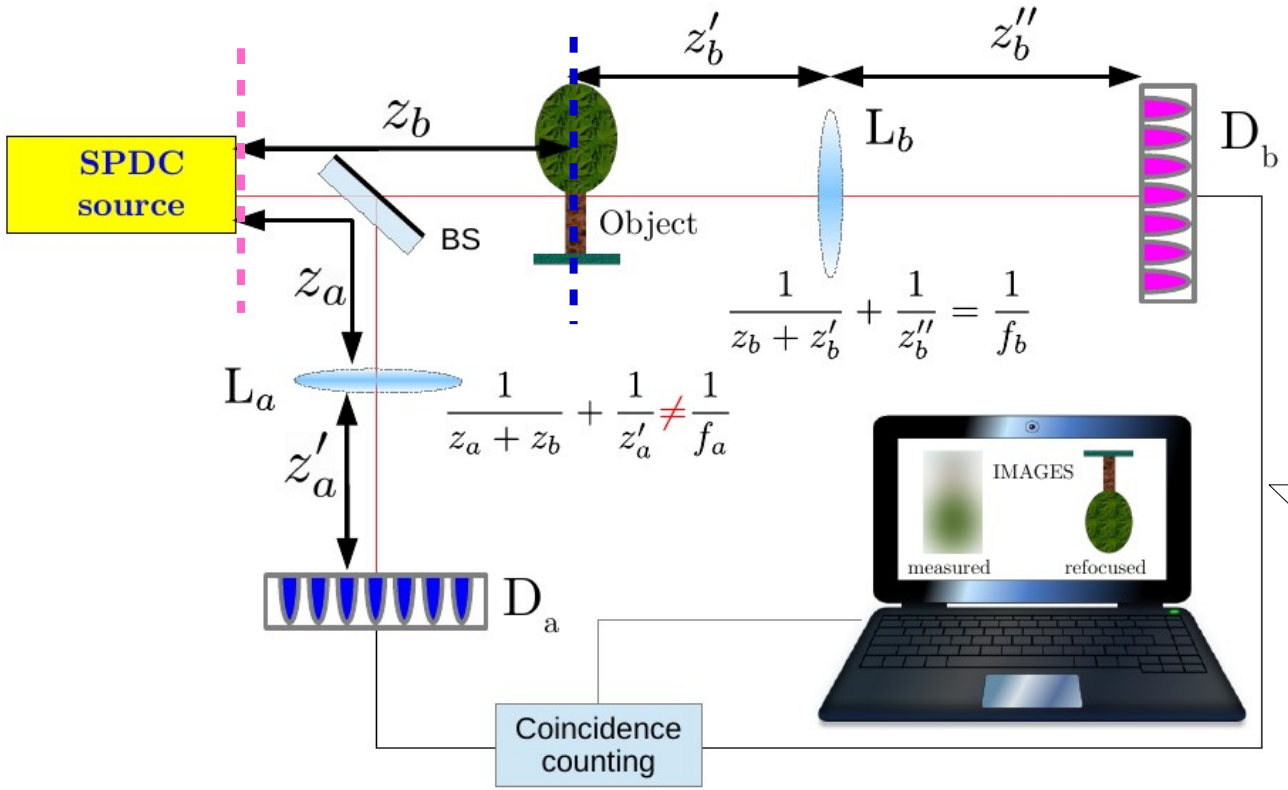

REFOCUS

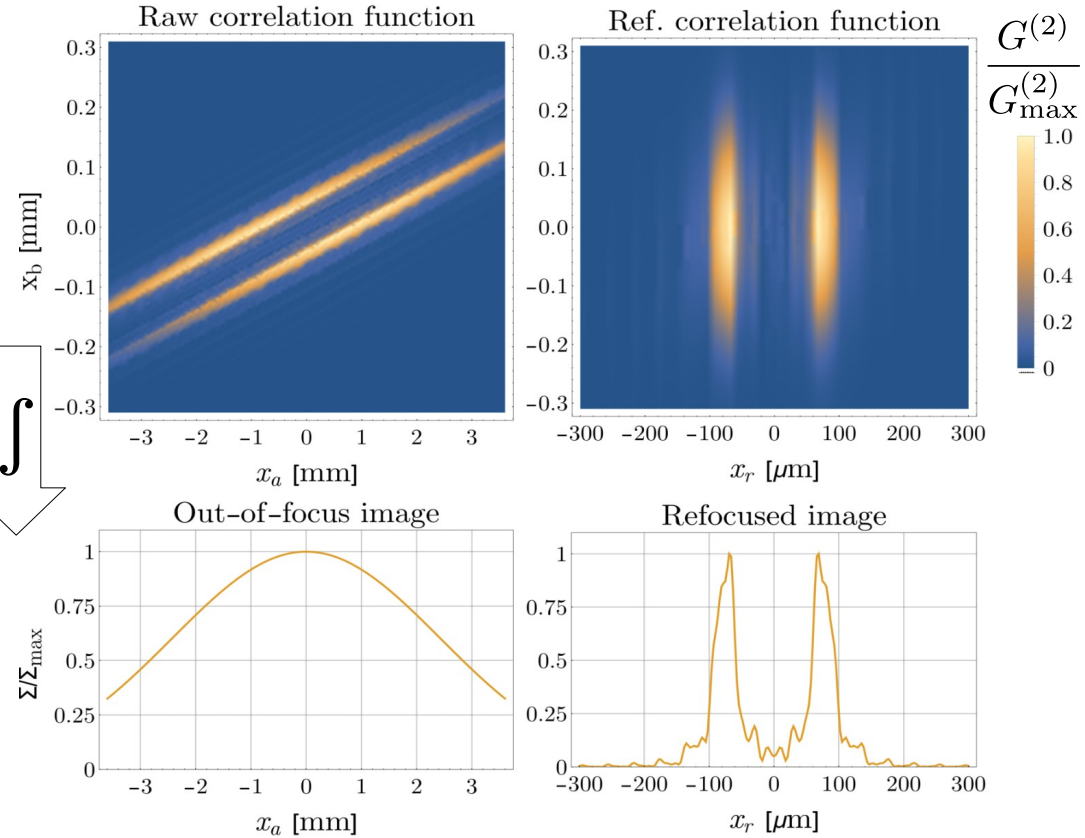

$$G^{(2)}(\rho_a, \rho_b; t_a, t_b) = < E_a^{(-)}(\rho_a, t_a) E_b^{(-)}(\rho_b, t_b) E_a^{(+)}(\rho_a, t_a) E_b^{(+)}(\rho_b, t_b) >$$

$E_j \rightarrow$ Field at the detectors

The second order correlation function is characterized by plenoptic properties

- F. V. Pepe, F. Di Lena, A. Garuccio, G. Scarcelli, and M. D'Angelo, Technologies, vol. 4, no. 2, p. 17, 2016

Appendix

Experimental correlation function

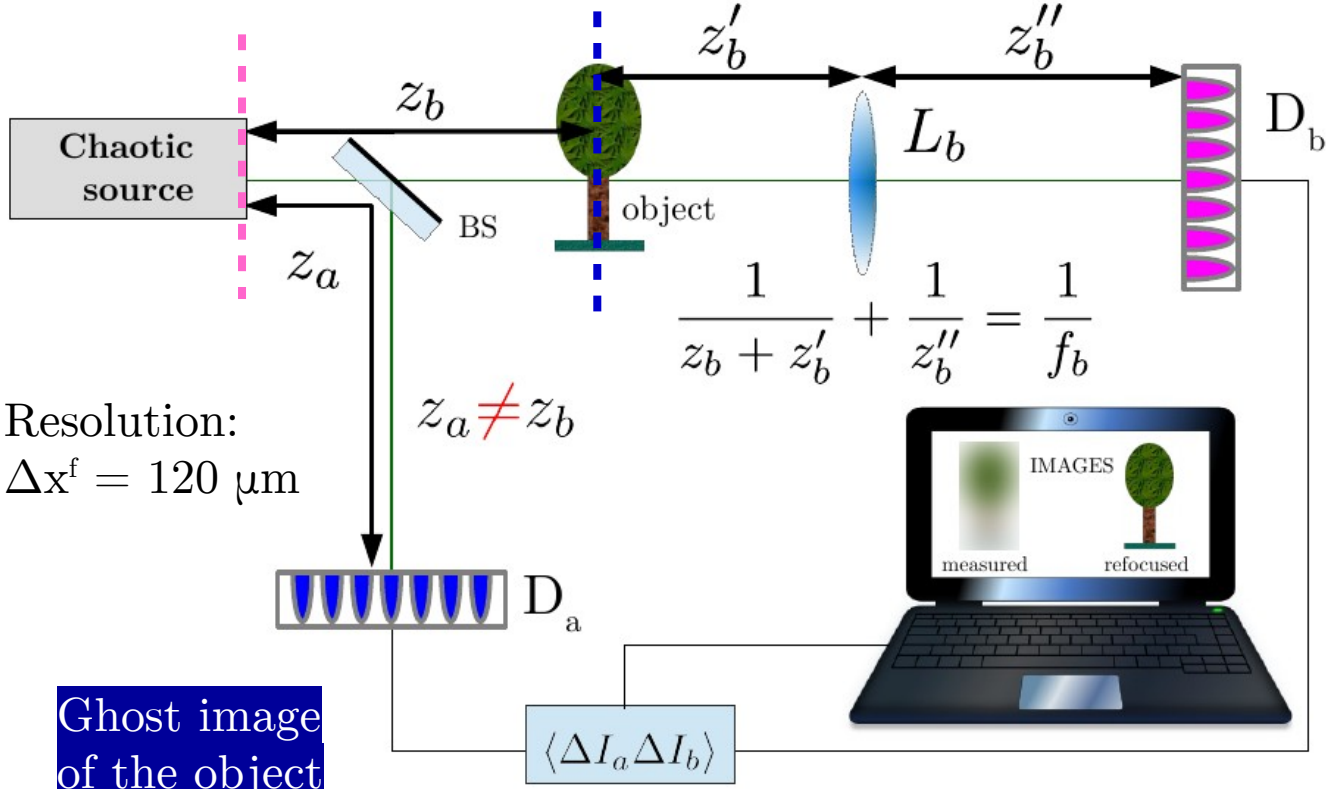

Resolution:
$\Delta x^f = 120\ \mu m$

Ghost image of the object

Standard image of the source

Object: double slit
D_a and D_b: scan. photodiodes

RAW data → Refocusing

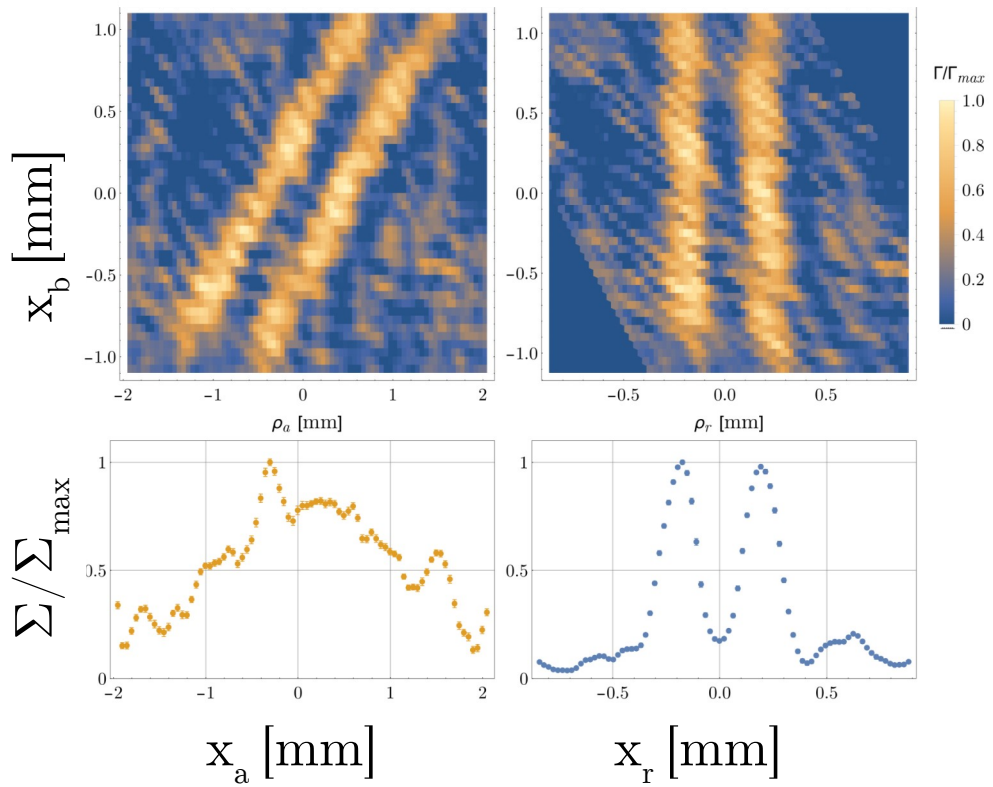

F. Di Lena, F. Pepe, A. Mazzilli, A. Garuccio, G. Scarcelli and M. D'Angelo, Nuovo Cimento C, vol. 41, 2018. Awarded talk @SIF 2017.

Appendix

Experimental correlation function

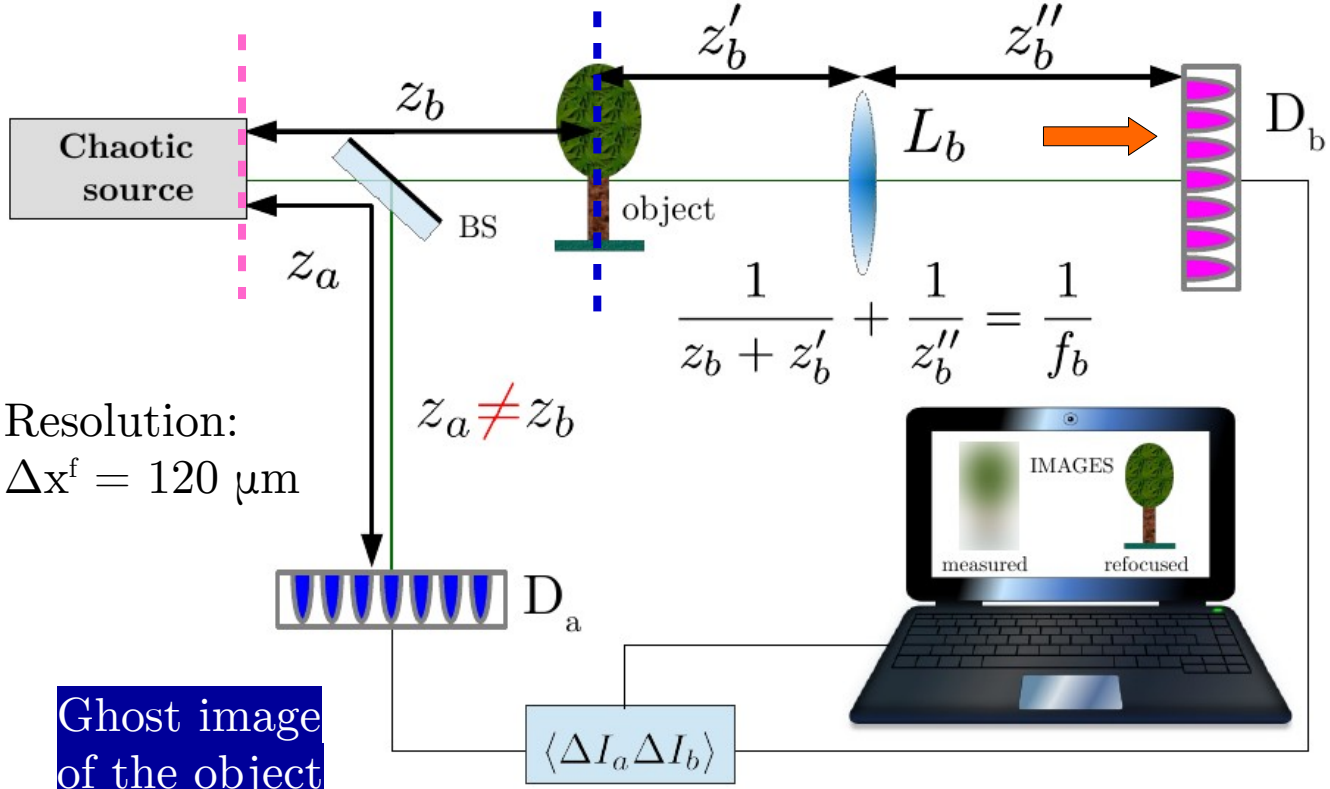

Resolution:
$\Delta x^f = 120\ \mu m$

Ghost image of the object

Standard image of the source

Object: double slit
D_a and D_b: scan. photodiodes

RAW data → Refocusing

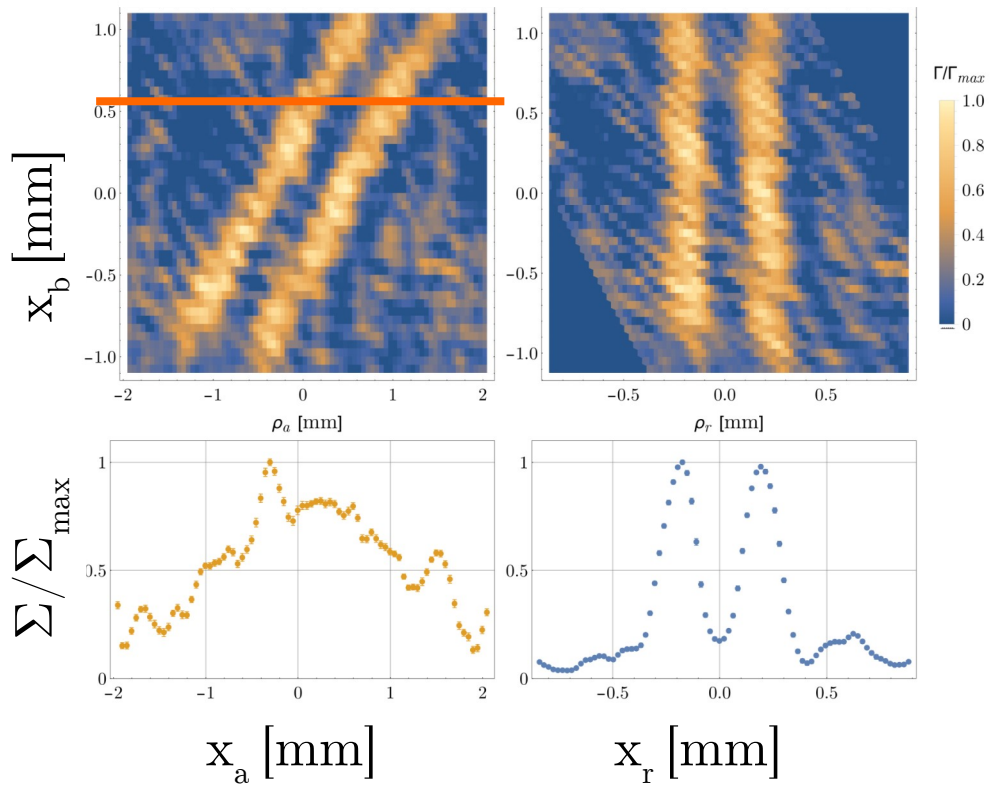

F. Di Lena, F. Pepe, A. Mazzilli, A. Garuccio, G. Scarcelli and M. D'Angelo, Nuovo Cimento C, vol. 41, 2018. Awarded talk @SIF 2017.

Appendix

CPI between arbitrary planes

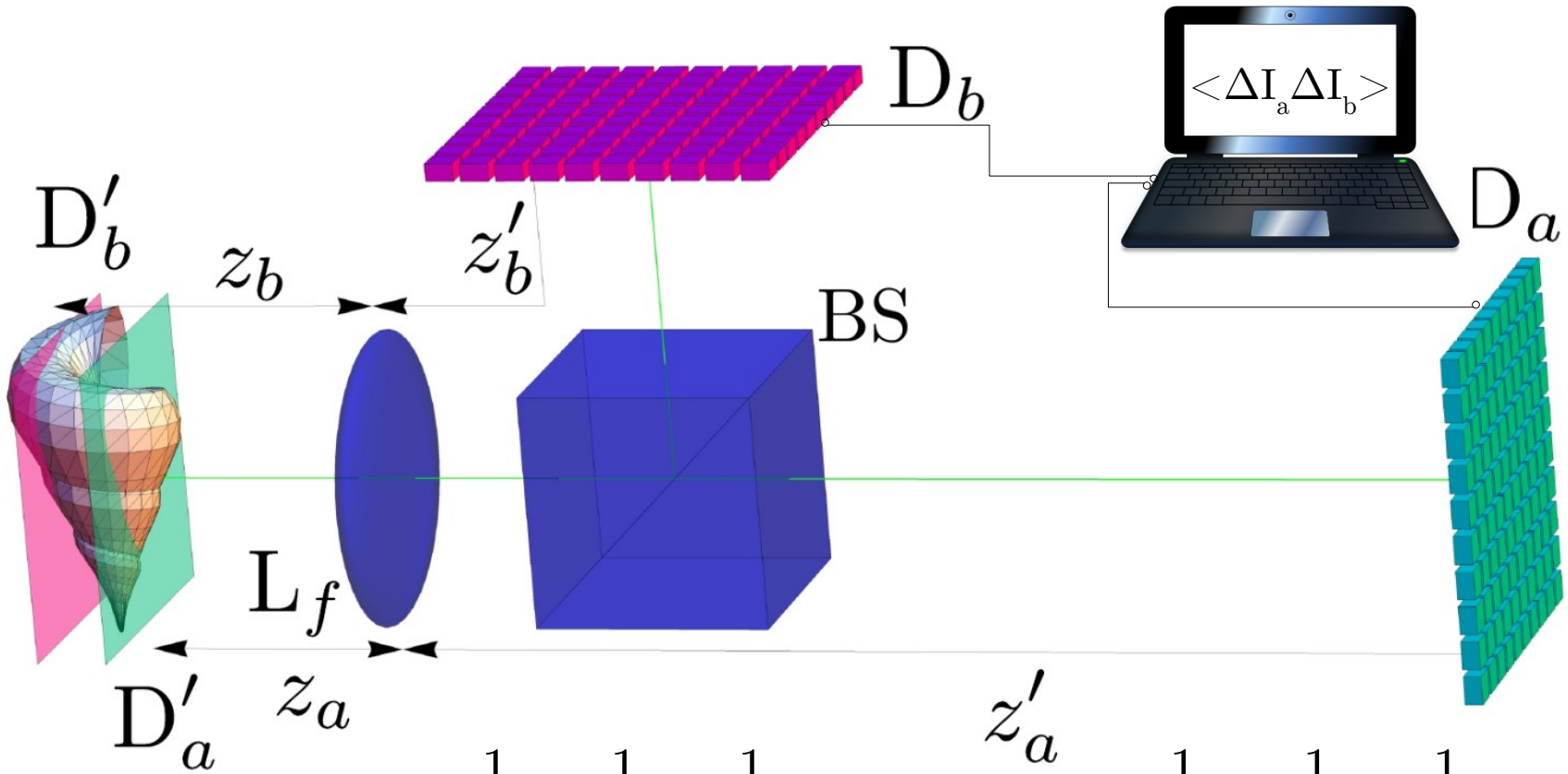

A light crossing both planes D'a and D'_b, within the 3D scene, is collected by both detectors D_a and D_b, and can thus be reconstructed.

- F. Di Lena, M. D'Angelo, F. V. Pepe, A. Garuccio, brevetto internazionale PCT/IB2019/052351 depositato il 22/03/2019.
- F. Di Lena, G. Massaro, A. Lupo, A. Garuccio, F. V. Pepe, and M. D'Angelo, Optics Express, vol. 28, n. 24, pp. 35857–35868, 2020.

Appendix

CPI between arbitrary planes

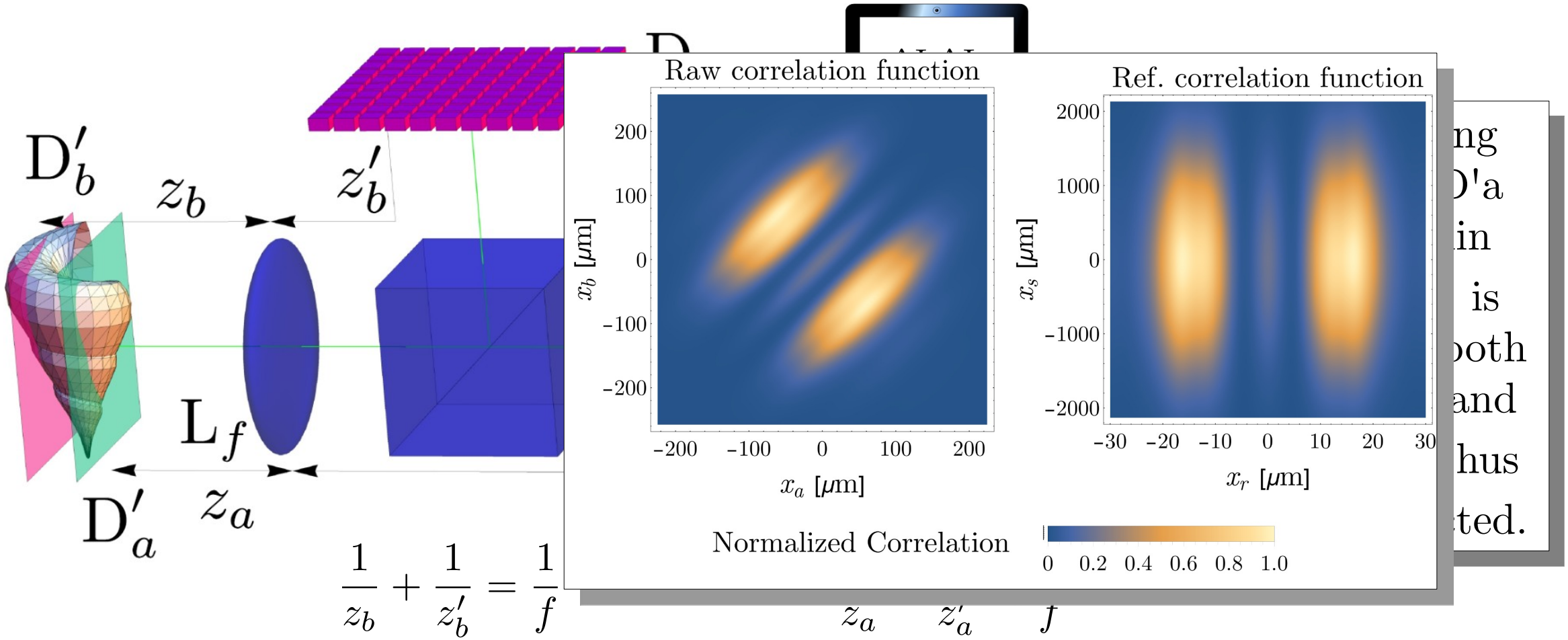

- F. Di Lena, M. D'Angelo, F. V. Pepe, A. Garuccio, brevetto internazionale PCT/IB2019/052351 depositato il 22/03/2019.
- F. Di Lena, G. Massaro, A. Lupo, A. Garuccio, F. V. Pepe, and M. D'Angelo, Optics Express, vol. 28, n. 24, pp. 35857–35868, 2020.

Appendix

CPI between arbitrary planes

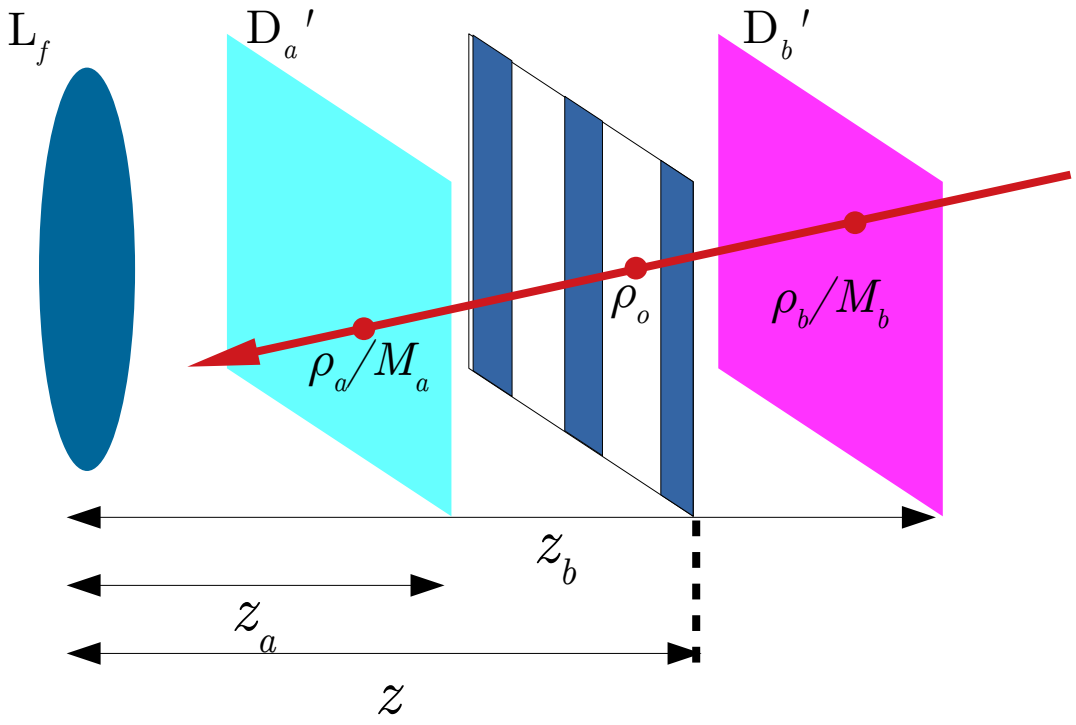

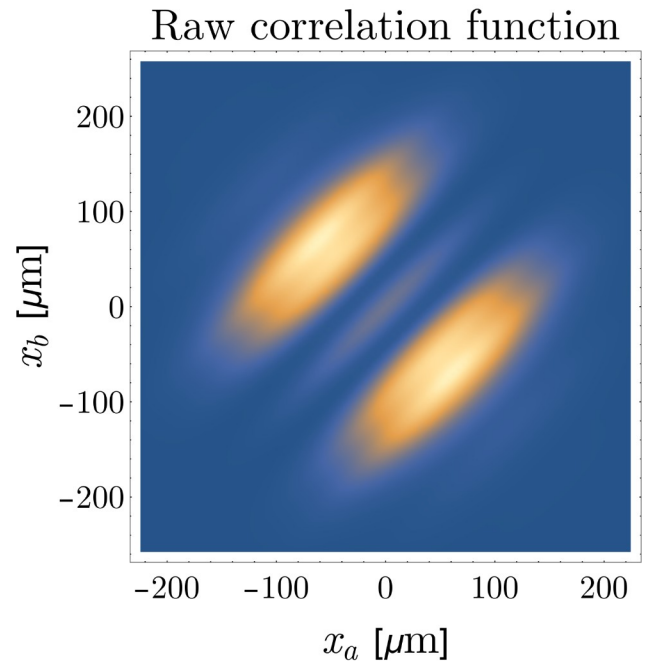

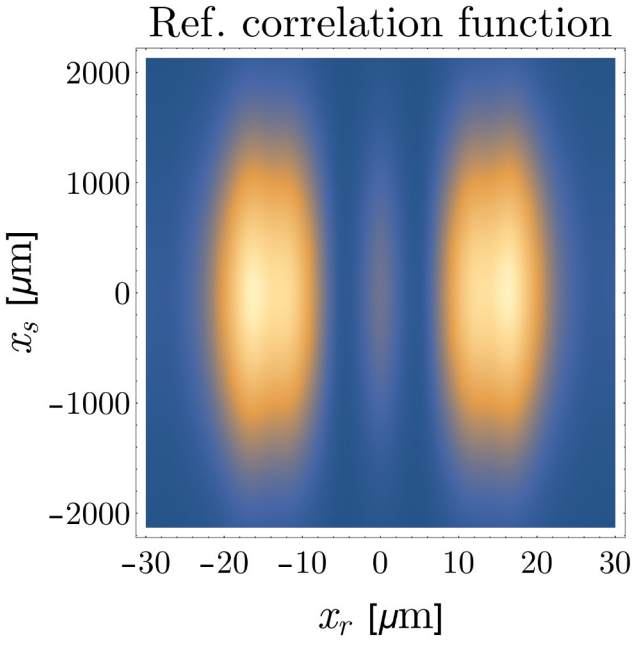

$$\rho_o \to \rho_r = \frac{1}{z_b - z_a}\left(\frac{z - z_a}{M_b}\rho_b + \frac{z - z_a}{M_b}\rho_b\right)$$

Patent request n.
M. D'Angelo, F. Di Lena, A. Garuccio, F. V. Pepe.

Appendix

DOF of CPI between AP

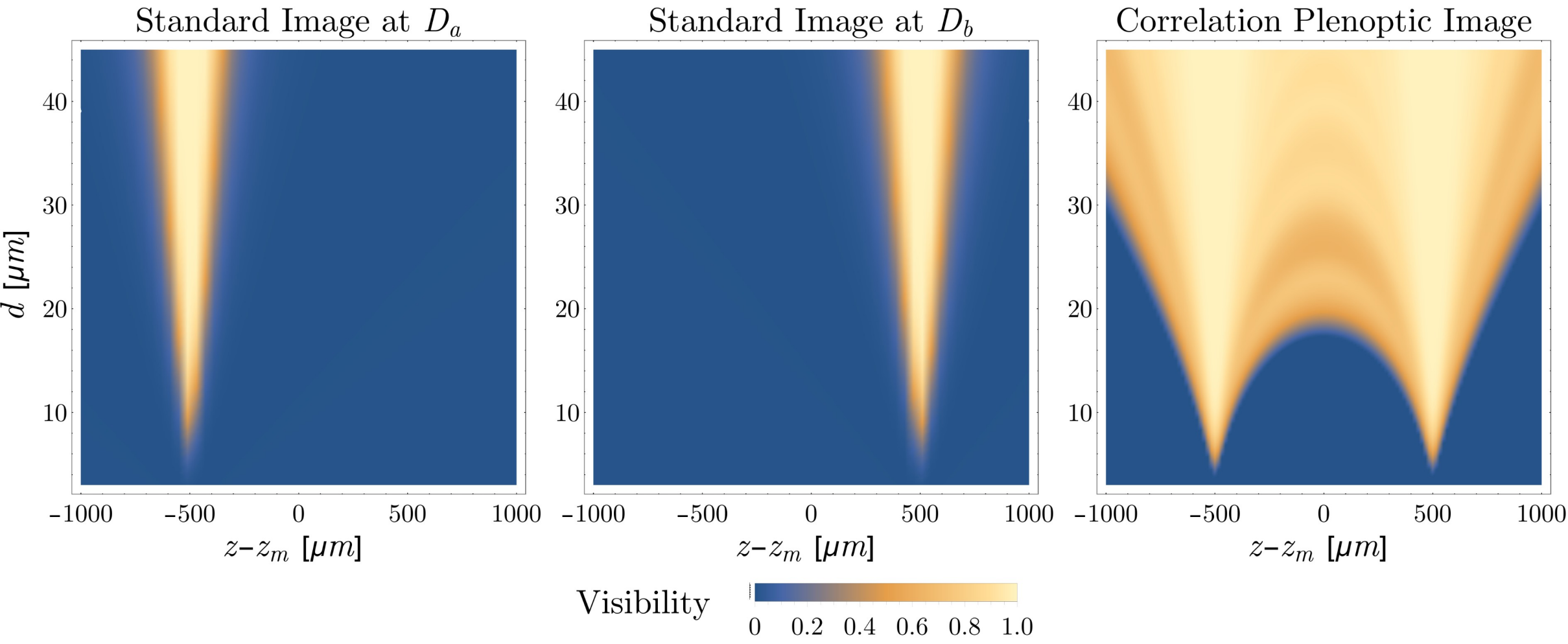

- F. Di Lena, M. D'Angelo, F. V. Pepe, A. Garuccio, brevetto internazionale PCT/IB2019/052351 depositato il 22/03/2019.
- F. Di Lena, G. Massaro, A. Lupo, A. Garuccio, F. V. Pepe, and M. D'Angelo, Optics Express, vol. 28, n. 24, pp. 35857–35868, 2020.

Advantage of entangled photons

Entangled photons enable sub-shot imaging

G. Brida, M. Genovese, and I. R. Berchera Nature Photonics, vol. 4, no. 4, pp. 227–230, 2010 @INRiM.

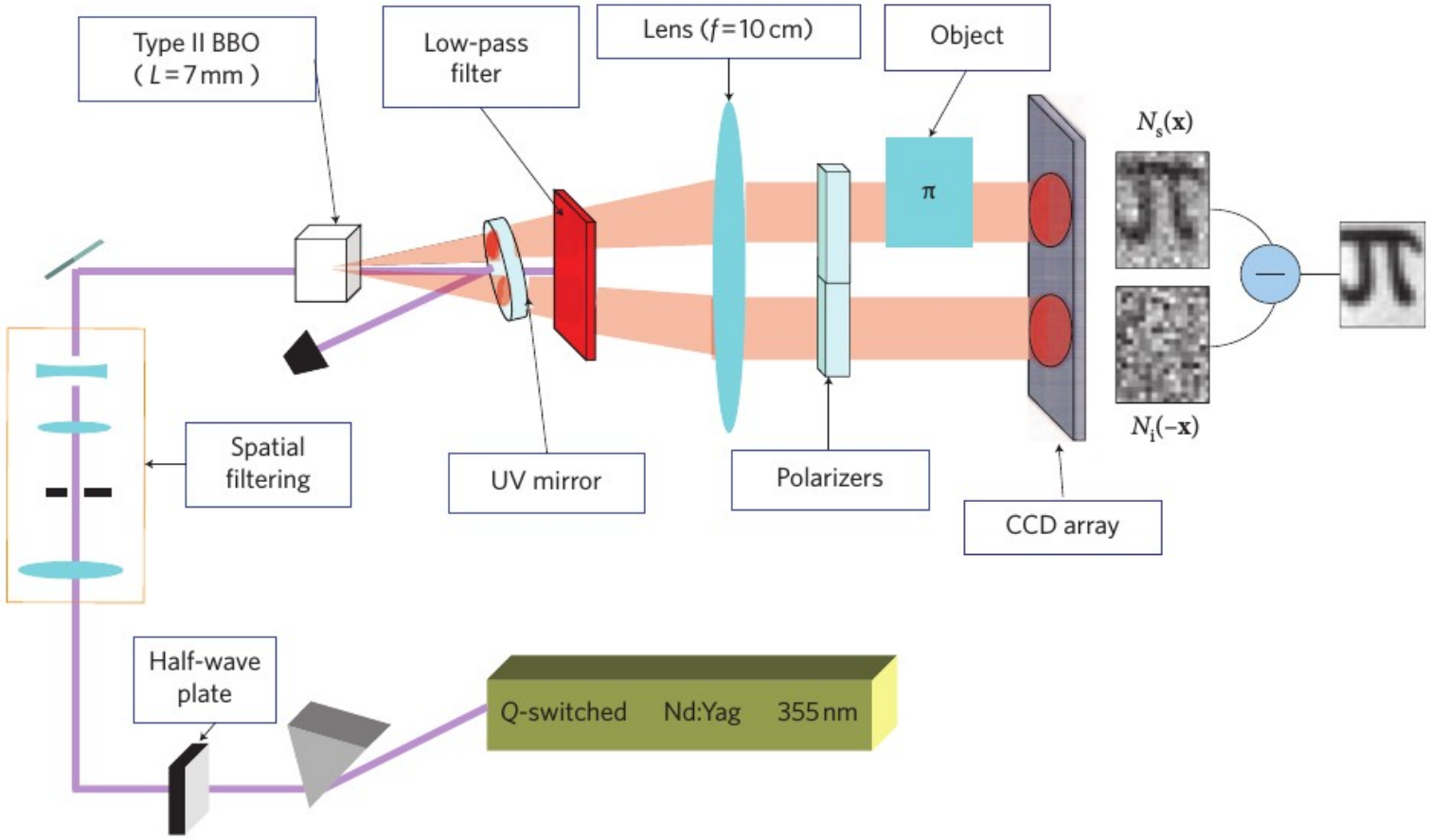

Application of entangled photons to optimize the SNR of CPI at low photons flux

- Biomedical and security application